2019

# The Role of IRF1 in the Brain and in Adaptive Responses of Astrocytes

Andrew Hoskins

THE ROLE OF IRF1 IN THE BRAIN AND IN ADAPTIVE RESPONSES OF ASTROCYTES

A thesis submitted in partial fulfillment of the requirements for the degree of Masters of Science

at Virginia Commonwealth University

by

ANDREW HOSKINS

Bachelors of Science, University of Virginia, 2017

Director: TOMASZ KORDULA

PROFESSOR, DEPARTMENT OF BIOCHEMISTRY AND MOLECULAR BIOLOGY

Virginia Commonwealth University

Richmond, Virginia

May, 2019

Acknowledgements

I would like to thank my advisor, Dr. Tomasz Kordula, and my committee members, Dr. Sarah Spiegel and Dr. Jeffrey Dupree. I would like to thank Tomek for allowing me to join his lab and for having to deal with my over-attention to detail at times. I would also like to thank my current and former lab members, Dr. LaShardai Brown, Dr. Debolina Biswas, Karli Mockenhaupt, and Mike Marone. Thank you for dealing with me asking a lot of questions at times and always providing a relaxed lab environment for me. It would not have been easy making it through this year with any other group of people. I would like to thank my parents, Richard and Elizabeth for their support over the years. I could not have made it to this point without their financial and emotional support. I would also like to thank my siblings, Jennifer and Emma for always being there if I needed someone to talk to. Last, and certainly not least, I would like to thank my friend Nathan Nayda for always housing me on my frequent trips up to DC when I needed an escape from stress over the past two years.

Table of Contents

List of Figures

Page

Abstract

THE ROLE OF IRF1 IN THE BRAIN AND IN ADAPTIVE RESPONSES OF ASTROCYTES

A thesis submitted in partial fulfillment of the requirements for the degree of Masters of Science at Virginia Commonwealth University

Virginia Commonwealth University, 2019

Major Director: Tomasz Kordula

Professor, Department of Biochemistry

In neurodegenerative diseases, the CNS becomes inflamed through activation of pathways, including the NF-κB pathway. Some of the therapies for those diseases target neuroinflammatory pathways. Here, we explore the mechanisms for the upregulation of a subset of genes following a restimulation of the NF-κB pathway. We discover that this upregulation occurs independent of IRF1 expression and type 1 interferon signaling. A knockdown of IRF1 using siRNA and an inhibition of JAK proteins using inhibitor AG490 both had no effect on priming. A secreted factor was found to upregulate the expression of both this subset of genes and genes encoding pro-inflammatory cytokines induced by NF-κB activation. We also explored the role of IRF1 in a mouse model of multiple sclerosis. We found that the deletion of IRF1 from oligodendrocytes diminished EAE severity. A deletion of IRF1 from myeloid cells within mice did not diminish EAE severity, however showed a promising decrease in the expression of certain inflammatory genes. Thus, IRF1 plays a critical role in fine-tuning inflammatory responses in the brain.

# CHAPTER 1

# INTRODUCTION

## Neurodegeneration

Neurodegenerative diseases are a highly prevalent epidemic in the world, occurring in multiple forms. The most common neurodegenerative disease, Alzheimer's Disease (AD), affects 24 million people globally (Reitz et al., 2011). Neurodegenerative diseases can cause a multitude of symptoms such as cognitive deficits in AD and motor deficits found in Multiple Sclerosis (Erkkinen et at., 2018). The innate immune system is responsible for the onset of these destructive diseases (Steinman, 2008). A major mediator of the immune response in the CNS is IL-1β and as expected, IL-1β is upregulated in patients with AD (Griffin et al., 1989). The mature form of IL-1β is a 153 amino acid, 17kDa peptide (March et al., 1985). It is a member of the IL-1 receptor and ligand family consisting of: IL-1α, IL-1β, IL-1ra, IL-1R1, IL-1RII, and AcP. IL-1β is a pro-inflammatory cytokine that is always present in the CNS, however in healthy individuals it is present at low concentrations (Basu et al., 2004).

## Sterile Inflammation

In a healthy brain, the blood brain barrier allows for enhanced protection of the tissue. The blood brain barrier is a term that describes the increased selectivity of the vasculature in the vessels of the brain (Dobbing, 1961). A typical blood vessel of the body features fenestrations that allows for transfer between the vessels and surrounding tissue. Since the CNS is such a vital system in the body, the blood brain barrier is non-fenestrated allowing for tight regulation of ion exchange and a prevention of invasion by any foreign microorganisms. This tight regulation allows for maintenance of a stable homeostasis in the CNS (Zlokovic et al., 2008). During infections and also sterile inflammation, the blood brain barrier becomes damaged, allowing for the penetration of the immune cells of the body (Banjara et al., 2017). Sterile inflammation is a type of inflammation that occurs without the introduction of a foreign microorganism to the area of inflammation. This process occurs during times where there is inadequate blood flow in response to tissue trauma. In neurodegenerative diseases, which feature high levels of sterile inflammation, the capillaries of the vasculature in the brain become shortened, resulting in a leaky and non-functional blood brain barrier. For this reason, sterile inflammation is characterized by a local recruitment of monocytes and neutrophils due to the breakdown of the blood brain barrier and the production of pro-inflammatory cytokines, including IL-1β and chemokines, such as CCL5 (Chen et al., 2010). These cytokines and chemokines, secreted by activated microglia and astrocytes, thus promote inflammation.

## Astrocyte Activation

IL-1β has the ability to activate both microglia and astrocytes, glia present in the CNS (Moynagh, 2005). Astrocytes are responsible for regulating the blood-brain barrier, maintaining ion homeostasis, controlling synapse formation, and many more functions, all which are affected

by astrogliosis that occurs during neurodegeneration (Sofroniew et al., 2010). Astrogliosis is the process in which astrocytes become reactive and begin to proliferate (Sofroniew, 2015). The neuroinflammatory effects in these reactive astrocytes are mediated through activation of transcription factor nuclear factor κB (NF-κB) and mitogen-activated protein kinases (Liu et al., 2017). Following the activation of inflammatory pathways, astrocytes secrete chemokines which attract immune cells to the area of inflammation, an event that can be harmful for the CNS (Ransohoff, 2002).

**NF-κB**

NF-κB is a crucial mediator of the inflammatory response in the brain. When NF-κB becomes dysregulated, as it does in some of the aforementioned neurodegenerative diseases, it can lead to the undesirable symptoms that come with these diseases (Liu et al., 2017). NF-κB refers to a group of transcription factors with similar structures. Members of NF-κB include p50 (NF-κB1), p52 (NF-κB2), p65 (RelA), RelB, and c-Rel. p52 is an NF-κB protein that is formed through the process of its precursor, p100 (Sun et al., 2013). During normal physiological conditions, NF-κB features a canonical pathway, mediated by p65/p50 complexes and a non-canonical pathway, mediated by RelB/p52 complexes. During NF-κB activation, these complexes form and translocate into the nucleus. When in the nucleus, they bind to specific regions of DNA and promote the expression of genes. The canonical pathway of NF-κB promotes genes of inflammatory cytokines and the non-canonical pathway promotes genes involved in lymphoid development (Millet et al., 2013).

Activation of NF-κB occurs following the binding of specific ligands to their receptor. The three common ligands that induce canonical activation are lipopolysaccharides (LPS), which bind to toll-like receptors (TLR), tumor necrosis factor alpha (TNF-α), which binds to the TNF receptor

(TNFR), and interleukin 1 beta (IL-1β), which binds to the interleukin 1 receptor (IL-1R). This leads to activation of IκB kinase beta (IKKβ) in the IKK complex. This activation leads to the phosphorylation of IκBα, which then gets polyubiquitinated and targeted for degradation. This degradation frees the p65/p50 complex and allows it to translocate to the nucleus and alter gene expression (Hoesel et al., 2013).

**RelB**

Following activation of the NF-κB pathway, it has been found that there is an increase in the concentration of RelB within the cell. After this increase, RelB begins to interact with the canonical NF-κB pathway (Hayden, 2012). Although RelB has a greater affinity for p52 than p50, at high concentrations of RelB, it can also be found binding to p50. These RelB/p50 complexes promote transcription of a unique set of genes, different from those promoted by p65/p50 complexes (Shih et al., 2012). In macrophages and dendritic cells, the induction of this RelB canonical pathway not only alters the gene expression of their unique set of genes, but also those genes promoted by p65/p50 complexes. These RelB/p50 complexes also inhibit p65/p50-induced pro-inflammatory cytokine induction (Gasparini et al., 2013).

**Interferon Regulatory Factor 1**

The human IRF family consists of 9 proteins, IRF1-9. All of the IRF proteins feature an N-terminal DNA binding domain that features a helix-turn-helix structure used to bind to an IFN-stimulated response element (ISRE) at the consensus sequence of 5′-AANNGAAA-3′. IRF1 is a 325 amino acid protein, encoded by a gene that can be found on chromosome 5q31.1. IRF1 features an IRF associated domain 2, shared by IRF2 (Yanai et al., 2012). IRF1 plays multiple roles downstream of IL-1β-induced activation of the NF-κB pathway. IRF1 is an NF-κB dependent gene that is induced during canonical activation. It has been found that IRF1 is crucial in the expression

of delayed IL-1β-responsive genes. IL-1β stimulation induces a K63-linked polyubiquitination of IRF1 by Baculoviral IAP repeat-containing protein3 (cIAP2) in the presence of sphingosine 1-phosphate (S1P). This results in the activation of IRF1, its translocation to the nucleus, and activation of IRF1-dependent genes, including those encoding chemokines CXCL10 and CCL5 (Harikumar et al., 2014). As previously stated, chemokines, such as CXCL10 and CCL5, attract immune cells to the area of inflammation. Along with its involvement in the expression of delayed genes, IRF1 has been found to play a role in the production of interferon beta (IFN-β), a signaling molecule that can activate the JAK-STAT pathway (Schmitz et al., 2007).

**JAK-STAT Pathway**

The JAK-STAT pathway is mediated by two sets of proteins, the Signal Transducer and Activator of Transcription (STAT) proteins and the Janus Kinase (JAK) proteins. The JAKs are comprised of four members, JAK1, JAK2, JAK3, and Tyk2. The JAKs each feature a FERM domain, that allows them to bind to their receptors, an SH2 domain, and a kinase domain, that allows them to phosphorylate nearby targets (Yamoaka et al., 1977). STAT proteins are a family of transcription factors that have a unique ability to transduce a signal from the membrane to the nucleus without the use of a secondary messenger. The first two proteins of this family to be discovered were STAT1 and STAT2, however since their discovery, five more have been identified. STAT proteins feature an N-terminal domain that allows them to form complexes with other STAT monomers, a coiled-coil domain involved in interaction with non-STAT proteins, a DNA binding domain, allowing them to alter gene expression, an SH2 domain that allows them to bind to receptors and also dimerize, a tyrosine residue that is the target for activation through phosphorylation, and a highly disordered transactivation domain that interacts with other proteins (Lim et al., 2006).

The JAK-STAT pathway can be activated by many cytokines, including IFN-β. Following the binding of IFN-β to the IFNR1, JAK phosphorylates the intracellular domain of the receptor, providing a site for the SH2 domain of STAT1 and STAT2 to bind. Following this binding, the proximity of the STAT proteins to the JAK bound to the receptor allows for JAK mediated phosphorylation of the tyrosine residue on the STAT proteins (Rawlings, 2004). This phosphorylation of STAT1 and STAT2 allows for a STAT1/STAT2 heterodimer to form, followed by a binding of IRF9 to the dimer to form the ISGF3 complex, which translocates to the nucleus in order to bind to the DNA at the promotors of genes, altering gene expression (Alturki et al., 2014).

There are other pathways that oppose this type 1 interferon induced activation. STAT3 is a protein that is activated by IL-6. IL-6 binds to the IL-6R on the cell membrane inducing the formation of 6-unit heteromeric complex including 2 molecules of IL-6, 2 molecules of IL-6R, and 2 molecules of a beta subunit of the IL-6R, known as gp130. As a result of this complex formation, STAT3 is phosphorylated through JAKs (Johnson et al., 2018). pSTAT3 has been found to be a negative regular of IRF1 signaling. As a result of STAT3 phosphorylation, the interferon producing effects of IRF1 are inhibited. This in turn leads to a decrease in type 1 interferon signaling (Zhou et al., 2019).

**Tolerant Genes**

The innate immune system of the body has an adaptive feature. The adaptivity of immune cells can be seen in the plasticity of gene expression following disease activation (Locati et al., 2013). The adaptivity of the immune system has been most explored in macrophages. Following activation by different ligands, macrophages alter their gene expression to fit closer to the profile of an M1, or classically activated macrophage, or an M2, or alternatively activated macrophage.

The type of activation that occurs is dependent on the ligand that activates the macrophage. Ligands such as IFN-γ and LPS will polarize a macrophage to fit an M1 profile, while ligands such as IL-4 and IL-13 will polarize a macrophage to fit an M2 profile (Biswas et al., 2012). Although macrophages polarize, the M1/M2 profile is all on a spectrum, and macrophages could express genes characteristic of both. The genes representative of M1 profiles include pro-inflammatory cytokines and inducible nitric oxide synthetase while the genes representative of M2 profiles include molecules from the arginase pathway and IL-10 (Biswas et al., 2010).

A concept of tolerance within macrophages was discovered where a re-stimulation with LPS produces different gene expression than an initial LPS stimulation. As stated before, LPS stimulation produces high expression of pro-inflammatory cytokines in macrophages, however interestingly, a second stimulation with LPS for the same macrophages lowers the expression of these cytokines (De Lima et al., 2014). The mechanism for tolerance in macrophages can be attributed to multiple factors. First, expression of negative regulators of TLRs were found at greater levels in the tolerant macrophages (Mages et al., 2008). This alone could not be the entire explanation for the tolerance, however, as some genes typically produced through LPS stimulation were not affected by the tolerance at the same levels. The main contributor to the tolerance was found to be epigenetic modification (Hoeksema et al., 2016). Through histone modification, specific promotors of genes can be targeted for downregulation, opposed to entire pathways. One model of macrophage tolerance showed that this silencing of pro-inflammatory cytokines is due to RelB mediated effects following NF-κB activation through TLR4 by LPS. The initial stimulation of NF-κB results in an increase of RelB concentration in the macrophages. RelB/p50 complexes were found to coordinate histone deacetylase SIRT1 and methyltransferase G9a. These

epigenetic regulators subsequently methylate H3K9, resulting in transcriptionally inactive promoters for the cytokine genes (Chen et al., 2009).

Recently, our lab has discovered that tolerance, like that seen in macrophages, occurs in astrocytes. When stimulated with IL-1β, human astrocytes develop a tolerance for a future stimulation with IL-1β. This tolerance can last for days and is characterized by a decrease in the gene expression when comparing an IL-1β stimulation of an IL-1β preconditioned astrocyte to an IL-1β stimulation of a naïve astrocyte. The tolerant genes that are controlled by this adaptive response are the pro-inflammatory cytokines that include IL-1β, IL-6, IL-8 and TNF-α. Originally, it was suspected that the tolerance in the astrocytes was due to a similar epigenetic mechanism that functions in macrophages; however, this was not the case. Upregulation of RelB following the initial stimulation with IL-1β activates the RelB canonical pathway and the RelB/p50 complexes bind to the tolerant genes. It was found that phosphorylation of S472 of RelB leads to a prolonged binding of the RelB/p50 complex to these promotors. When another stimulation with IL-1β occurs within days of this phenomenon, the RelB/p50 complexes block the p65/p50 complexes, which promote the expression of these cytokines, from binding to the cytokine promotors. This leads to lower expression of the cytokines (Gupta et al., in press).

**Primed Genes**

Another set of genes have been identified in astrocytes that show an opposite effect to that of the tolerant genes. These genes, coined the "primed" genes, when restimulated with IL-1β show an upregulation in their gene expression. These genes include LCN2, YKL-40, and CH25H. Lipocalin 2 (LCN2) is a protein secreted by astrocytes during neuroinflammation. LCN2 serves many functions during neuroinflammation, including the control of morphological changes in the astrocytes and the control of astrocyte survival or astrocyte death (Lee et al., 2015). LCN2 also

has been found to promote neuronal death and trigger insulin resistance in the CNS (Song et al., 2018). YKL-40, as its name suggests is a 40kDa glycoprotein that features a tyrosine, lysine, and leucine at its N-terminus (Kjaergaard et al., 2016). YKL-40 is highly expressed in many neurodegenerative diseases, including Alzheimer's disease (Bonneh-Barkay et al., 2010). YKL-40 can be used as a marker for astrocyte activation during times of neuroinflammation (Llorens et al., 2017). YKL-40 has also been found to upregulate VEGF expression in a glioblastoma cell line (Francescone et al., 2011). Cholesterol 25-hydroxylase (CH25H) is an IFN-stimulated gene that is responsible for the production of 25-hydroxycholesterol (25-HC). 25-HC is responsible for feedback inhibition of IL-1β-induced inflammation (Reboldi et al., 2014).

Recently, our lab has shown that priming does occur in human astrocytes. Through the use of siRelB, it was demonstrated that priming is RelB dependent. Western blot analysis showed that following activation of human astrocytes using IL-1β, within 15 minutes, p65/p50 NF-κB activation was seen. This was also correlated with an upregulation in phosphorylation of the IKKβ. Phosphorylation of the IKKβ leads to degradation of IκBα and this degradation could be detected through the disappearance of phosphorylated IκBα, also 15 minutes following stimulation. An hour after the IL-1β stimulation, IRF1 expression is induced. The accumulation of IRF1 occurred entirely in the nucleus, with no evidence of IRF1 found in the cytosol. This IRF1 expression led to an increase of IFN-β and subsequently activation of type 1 interferon signaling, detected through phosphorylation of STAT1 and STAT2. This delayed JAK-STAT signaling occurred 4 hours post IL-1β stimulation.

**Figure 1: IL-1β induced NF-κB activation results in type 1 interferon signaling.** (A) Following stimulation with 20ng/mL IL-1β, NF-κB activation can be seen within 15 minutes through western blotting using anti-IKK and anti-IκBα antibodies. (B) This NF-κB activation results in induction of IRF1, as seen in the western blot using anti-IRF1 antibodies. (C) Astrocytes were stimulated with 20ng/mL IL-1β for 2 hours and both the nuclear and cytoplasmic lysates were analyzed by western blotting using anti-IRF1 antibody. (D) Astrocytes were transfected with a CCL5 reporter and renilla expression plasmid, stimulated with 20ng/mL IL-1β for 8 hours, and luciferase activity and renilla activities were analyzed, * = $P < 0.05$. (E) qPCR analysis was performed on astrocytes following a 3-hour stimulation with 20ng/mL IL-1β and the expression of IFN- β was normalized to expression of GAPDH. (F) Astrocytes were stimulated with 20ng/mL IL-1β and their lysates were analyzed through western blotting using anti-pSTAT1 and anti-pSTAT2 antibodies. All of this work was performed by Lauren Bryan.

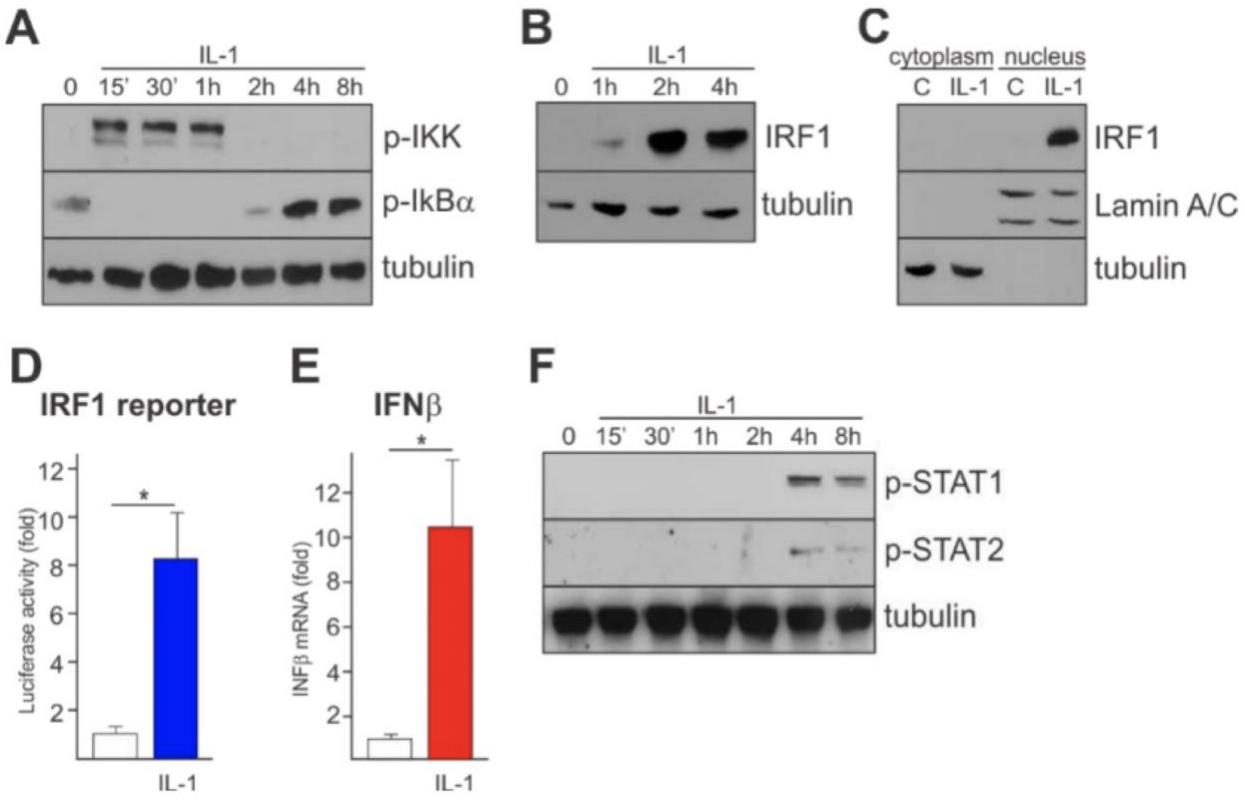

**Figure 2: Priming is mediated by IRF1 induced interferon signaling.** This proposed mechanism shows that activation of NF-κB results in an increase in IRF1 and RelB protein levels. IRF1 induction results in upregulation of IFN-β, which is secreted from the cell. In addition to this, IRF1 promotes the expression of genes required for priming to occur. IFN-β found adjacent to the astrocyte binds to the IFNR1, resulting in formation of the ISGF3 complex. The ISGF3 complex translocates to the nucleus promoting the expression of more genes required for priming to occur.

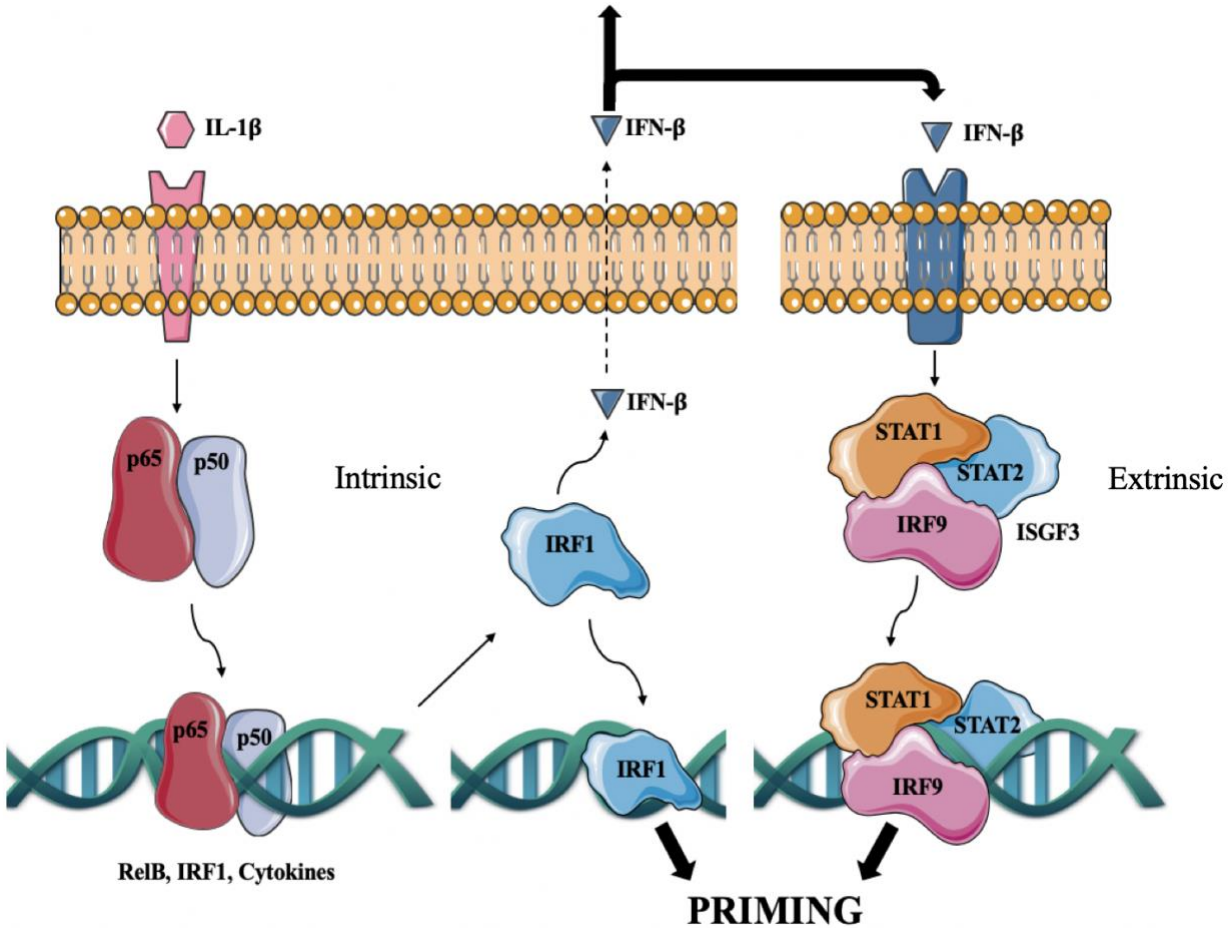

## Hypothesis

Priming is a phenomenon that results in the upregulation of a subset of genes following a second stimulation with IL-1β. Although we showed that priming occurs for the LCN2, YKL-40, and CH25H genes, it is not understood how this occurs. Our lab has shown that priming is RelB dependent mechanism similar to tolerance, however conversely in priming, it is likely that the DNA of the gene promotors will become more accessible, allowing their upregulation. Following IL-1β stimulation, IRF1 promotes the secretion of IFN-β leading to type 1 interferon activation. We theorize that the mechanism for making the LCN2, YKL-40, and CH25H promotors more accessible relies on both IRF1 and interferon signaling. In addition, we explored the importance of IRF1 in a model of multiple sclerosis, experimental autoimmune encephalitis (EAE). Since astrocyte specific deletion of IRF1 had limited effects in this model, we examine the role of oligodendrocytes and macrophages/microglia. We expected that the deletion of IRF1 will decrease the severity of the EAE treatment in both of these knockout models. The aim of this thesis is to determine if IRF1 signaling controls the upregulation of primed genes and also to determine the role that IRF1 plays in vivo during EAE.

## Materials and Methods

**Cell culture and reagents:**

Human cortical astrocytes were prepared from fetal tissue provided by Advanced Bioscience Resources and were cultured as previously described (2,3). Astrocyte cultures were prepared in Dulbecco's modified Eagle's medium (DMEM) supplemented with 10% fetal calf serum, Penicillin/Streptomycin, and non-essential amino acids. Cells were kept at 37℃ with 5% $CO_2$.

**Priming experiments:**

Human fetal astrocytes, after reaching 95% confluency in T75 flasks were removed using Trypsin and plated on 4 wells of a 6 well plate. The cells were given 2 mL of DMEM supplemented with 10% fetal calf serum, Penicillin/Streptomycin, and non-essential amino acids. When the cells grew to appropriate confluency (50%-75%), the $2^{nd}$ and $4^{th}$ wells were stimulated for 24 hours with 20ng/mL of IL-1β. Following the 24 hours, all wells were extensively washed with phosphate buffered saline (PBS) with a pH of 7.4 and given new media. 48 hours following the addition of new media to the cells, the $3^{rd}$ and $4^{th}$ wells were stimulated for 8 hours with 20ng/mL of IL-1β. At the end of the 8 hours, the wells were washed with PBS and treated with 1mL of Trizol.

**siRNA Transfection:**

Human fetal astrocytes were plated in 8 wells between two 6 well plates. Three mastermixes were made containing: A) 8uL 20uM human IRF1 siRNA (Dharmacon), 1mL 1x siRNA buffer (4.48mg/mL KCl, 1.44mg/mL HEPES, 0.04 mg/mL $MgCl_2 \cdot 6H_2O$, pH 7.3-7.6), 1mL serum free DMEM, B) 8uL 20uM Non-Targeting #1 siRNA (Dharmacon), 1mL 1x siRNA buffer, 1mL serum free DMEM, C) 32uL DharmaFECT1 in 4mL serum free media. These mastermixes were incubated at room temperature for 5 minutes, and then 2mL of mastermix C

was added to both mastermixes A and B. These mixtures resulting in 40uM siRNA were allowed to incubate for 20 minutes. 1mL of mixture A/C were added to 4 wells of plated fetal human astrocytes and 1mL of mixture B/C were added to the other 4 wells. 2 hours following this addition, the priming experiments were performed on all 8 wells (same conditions for each group of 4 wells). Astrocytes were plated in two 6cm dishes at the same time to analyze if the siRNA was properly functioning. These two dishes (one with A/C mastermix and one with A/B mastermix) were stimulated with 20ng/mL IL-1β for 1 hour and their RNA was collected.

**JAK Inhibition:**

Eight wells of astrocytes were plated across two 6 well plates. Four of the wells were treated with 50uM AG490 (Calbiochem) 30 minutes prior to their initial IL-1β stimulation and the other four were left untreated. Astrocytes were plated in four 6cm dishes and the 1$^{st}$ and 2$^{nd}$ dishes were given 50uM AG490. Following 30 minutes, the 2$^{rd}$ and 4$^{th}$ dishes were treated with 20ng/mL IL-1β for 4 hours and the protein of the four samples were collected to assure inhibition.

**RNA isolation:**

Trizol samples from the previously described experiments were stored at -80℃ after shaking. The 1 mL samples were treated with 200uL of chloroform and the mixture was centrifuged at 13,200 RPM for 15 minutes at room temperature. 500uL of the upper phase was transferred to new centrifuge tubes and 100uL of chloroform was added. Following another round of centrifuging at the same conditions, 400uL of the upper phase was transferred to new tubes. 1uL of molecular grade glycogen was added to the tube and the tubes were mixed. Following the addition of 500uL isopropanol, the tubes were gently inverted and placed on ice for 10 minutes. The tubes were centrifuged at 13,200 RPM for 10 minutes at 4℃ and the supernatant was poured off. 1mL of cold 70% ethanol was added to each tube and they were centrifuged at 13,200 RPM

for another 10 minutes at 4℃ and the supernatant was poured off again. This process was repeated one more time with another 1mL of cold 70% ethanol and the leftover ethanol was pipetted out of the tube. The tubes were placed at 37℃ to allow any final leftovers of ethanol to evaporate from the tube. The RNA pellets were resuspended in 22uL of $H_2O$ treated with DEPC.

**RT qPCR:**

Following the isolation, 1ug of the RNA was reverse-transcribed using a High Capacity cDNA Archive kit (Applied Biosystems). 1:10 and 1:100 dilutions of the resulting cDNA were made. 5uL of 1:100 cDNA was added to 4uL $H_2O$, 1uL of GAPDH SYBR primer (Bio-Rad) and 10uL of PowerUp SYBR Green Master Mix (Applied Biosystems). These mixtures were analyzed using a CFX Connect Real Time System Thermal Cycler (Bio-Rad). The samples were held at 95℃ for 30 seconds to start. The samples were then cycled from 95℃ for 10 seconds down to 60℃ for 30 seconds. The plate was read and the cycle was repeated 39 more times. GAPDH expression was used to normalize the fold induction of the genes of interest. The genes of interest were measured in the same manner, but using the 1:10 dilutions. The genes measured for the human samples were IL-1β, IL-6, IL-8, LCN2, YKL-40, CH25H, and TNF-α. The genes measured for mouse samples were IL-1β, IL-6, IL-8, IL-10, IL-17, LCN2, YKL-40, TNF-α, IFN-γ, CCL2, CCL5, CXCL10, CCR2, CD44, CD86, iNOS, Arg1, Olig2, MBP, PLP1, SiglecH, CX3CR1, CSF1R, and GFAP.

**Preparation of non-denaturing whole cell lysates:**

The cells plated from the JAK inhibitor experiment were stimulated as describe in the JAK inhibition protocol. The dishes were washed twice with PBS at the end of the experiment and 500uL of RIPA buffer (10mM Tris pH 7.4, 150mM NaCl, 0.5mM EDTA pH 8, 0.5% NP-40, 1% Triton X-100, 1mM NaV, 1mM complete protease inhibitor cocktail, 4mM PMSF). Each dish was

scraped and the RIPA buffer from each was collected. These samples were sonicated 10 times in short bursts, using a Sonic Dismembrantor Model 100 (Fischer). These lysates were centrifuged at 14,800 RPM for 5 minutes and the supernatants were collected. The lysates were stored at -80℃.

**BCA assay:**

A mastermix containing 98% BCA reagent A and 2% BCA reagent B (Thermo Fischer) was prepared. 995uL of the mastermix was added to 5uL of each lysate. These mixtures along with a 1mL blank of pure mastermix were incubated on a 55℃ heating block for 30 minutes. The $A_{280}$ of the resulting samples were read and the absorbance was converted to concentration using the formula $[sample] = \frac{A_{280}+0.1688}{0.0935*5}$.

**Western Blotting:**

For smaller proteins, 10% polyacrylamide gels were used and for larger proteins, 8% polyacrylamide gels were used. After assembling the gel, 40ug of each protein sample were put into a tube based on the concentration found from the BCA assay and $dH_2O$ was added to reach equal volumes in each tube. Loading buffer (98% Laemmli buffer mixed with 2% 2-mercaptoethanol) (Bio-Rad) was combined with each sample at a 1:1 ratio. These mixtures were boiled at 95℃ for 5 minutes and the samples were spun down at room temperature. The gels were washed with $dH_2O$, and the samples were loaded in each lane alongside a well with 10uL of Precision Plus Protein Dual Standards ladder (Bio-Rad). A 1:1 mixture of loading buffer:$dH_2O$ were added into each well that was not used. Running buffer (25mM Tris, 200mM glycine, 3.5mM sodium dodecyl sulfate) was used to fill the remainder of the space left in the wells and surrounding the anode and cathode. While in the stacking gel, samples were run at a voltage of 120V and while in the resolving gel, it was run at a voltage of 180V. Once the ladder showed that the gel had run

the appropriate distance, the gels were transferred for 15 minutes at 25V to a nitrocellulose membrane using 20mL Trans-Blot Turbo 5x Transfer Buffer (Bio-Rad), 20mL ethanol, and 60mL $dH_2O$ in a Trans-Blot Turbo Transfer System. Following a wash of the post-transfer nitrocellulose membrane, Ponceau stain (1% acetic acid with Ponceau powder) was applied to visualize total protein on the membrane. The membranes were washed using TTBS (150mM NaCl, 10mM Tris pH 8, and 0.1% NP-40). The membranes were blocked using 5% bovine serum albumin (2.5g BSA in 50mL TTBS) for 1 hour at room temperature. The membranes were incubated with their primary antibody overnight at 4℃. The antibodies used during my project were Tubulin (Santa Cruz), pSTAT1 (Cell Signaling), and pSTAT2 (Cell Signaling). The following day they were washed three times with TTBS and incubated with rabbit secondary antibody for an hour. They were then washed and exposed using Clarity Western ECL (Bio-Rad).

**Experimental Autoimmune Encephalomyelitis**

The mice received subcutaneous 200μg MOG35–55 peptide (AnaSpec) emulsified in CFA containing 200μg Mycobacterium tuberculosis H37Ra (Difco) and intraperitoneal 200ng pertussis toxin (Enzo Life Sciences). A booster dose of 200 ng pertussis toxin was administered 2 days after immunization. Mice were clinically scored and weighed daily, and the severity of the disease was quantified using a five-point scale: 0, no symptoms; 1, limp tail; 2, limp tail with loss of righting; 3, paralysis of single hind limb; 4, paralysis of both hind limbs; and 5, death.

## Results

**Priming occurs in human astrocytes.**

The first step to determining the mechanism of priming was to assure that this phenomenon does in fact occur in human astrocytes. All of the priming data shown was performed using the same stimulation schedule seen in Figure 1. The changes in expression were significant for each gene when comparing mRNA expression from pretreated IL-1β stimulated cells to naïve IL-1β stimulated cells. This value showed a 1.8-fold increase for LCN2 mRNA, a 2.5-fold increase for YKL-40 mRNA, and a 1.4-fold increase for CH25H mRNA. Interestingly, the control pretreated cells showed high levels of each gene expression even after they had not been treated with IL-1β for 56 hours. This shows that the expression of these genes is a long-lasting effect. This delayed expression was the greatest in YKL-40 mRNA, which showed a 4.1-fold change between the gene expression in control naïve cells and control pretreated cells. In LCN2 and CH25H gene expression, there was a 3.6-fold increase and 2.5-fold increase respectively for these same values.

**Figure 3: Upregulation of LCN2, YKL-40, and CH25H mRNAs occurs following a restimulation with IL-1β.** qPCR analysis was performed on the cDNA of human astrocytes following treatment with IL-1β based on the schedule shown below. Data shown is normalized to GAPDH and the IL-1β stimulated naïve cells were set to a fold induction of 100. P-values shown are based on a two-way t-test. LCN2 (n = 5), YKL-40 (n = 5), and CH25H (n = 3) mRNAs all showed significant increases in their expression when comparing the IL-1β stimulated pretreated cells to the IL-1β stimulated naïve cells.

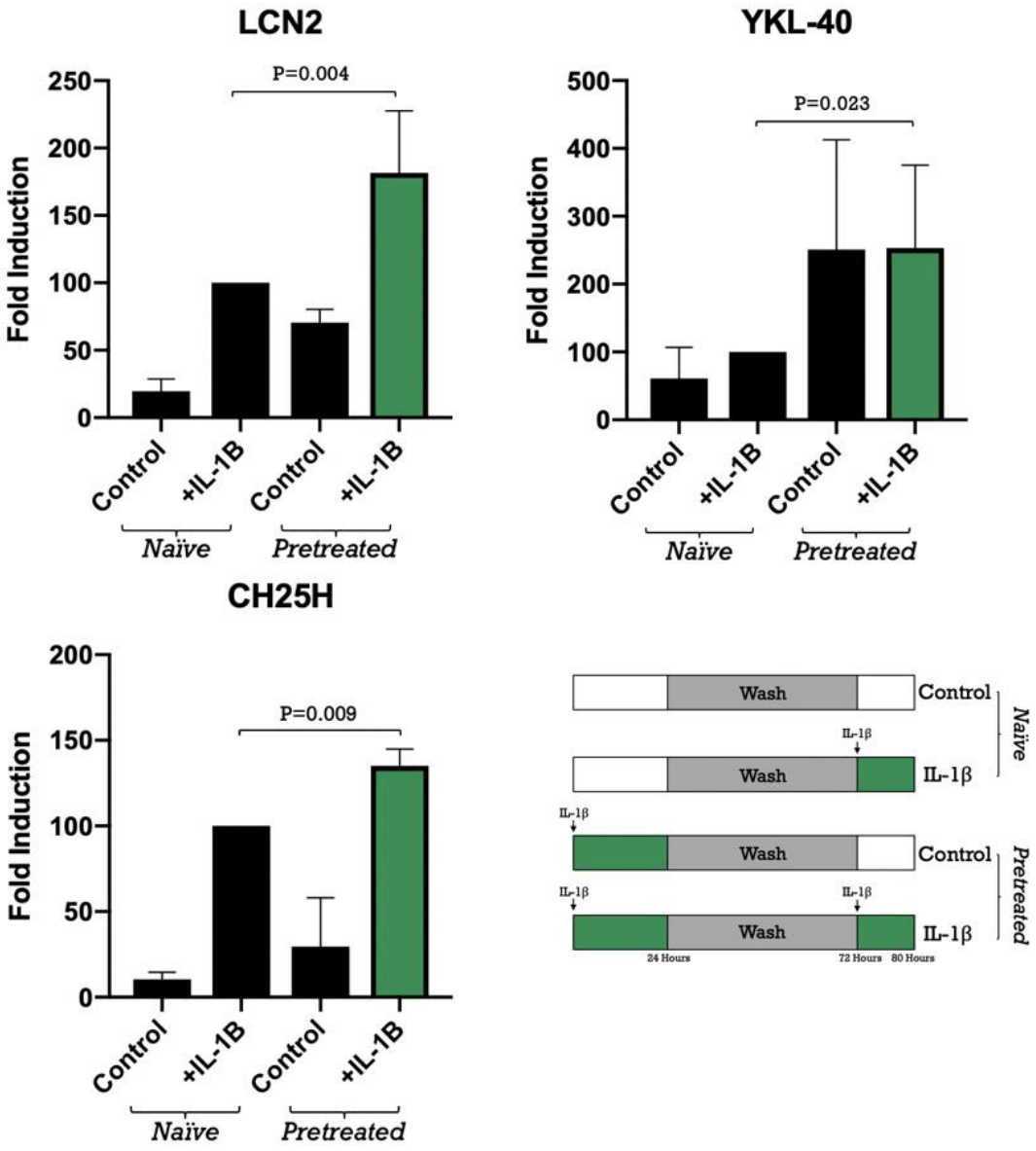

**Priming is IRF1 independent.**

In order to determine if priming was dependent on IRF1, its expression was knocked down. In this experiment, both IRF1 siRNA and control siRNA were used to compare the expression of the primed genes. The first step was to ensure that the IRF1 siRNA transfected cells were expressing lower amounts of IRF1 than the control siRNA transfected cells. The cells transfected with IRF1 siRNA expressed about 50% of the IRF1 mRNA compared to the control siRNA transfected cells (Figure 4). This showed that expression of IRF1 was in fact being knocked down. The four conditions previously used during the priming experiments were repeated, but this time using cells transfected with either control siRNA or IRF1 siRNA, leading to a total of eight conditions. According to the hypothetical mechanism that was propsed, IRF1 would both directly affect the gene expression responsible for priming through translocation to the nucleus and subsequent binding to the DNA along with indirectly affecting gene expression through type 1 interferon activation. If this was the case, the gene expression should show less of a priming effect between the two types of siRNA transfections. The ratio of gene expression in the naïve IL-1β stimulated cells to the pretreated IL-1β stimulated cells should be lower in the IRF1 siRNA treatment. However, statistically similar ratios of expression for LCN2, YKL-40, and CH25H mRNAs were observed in control and IRF1 knockdown astrocytes, suggesting that IRF1 is not required for priming (Figure 5).

**Figure 4: IRF1 siRNA results in a knockdown of IRF1 expression.** Cells were transfected with either IRF1 siRNA or control siRNA for 2 hours. Subsequently, cells were then stimulated with IL-1β for 1 hour. The cells were collected and IRF1 expression was analyzed using qPCR. Data shown is normalized to GAPDH expression and the values are shown compared to the IRF1 expression in control siRNA, which was set to a value of 1 (n = 1).

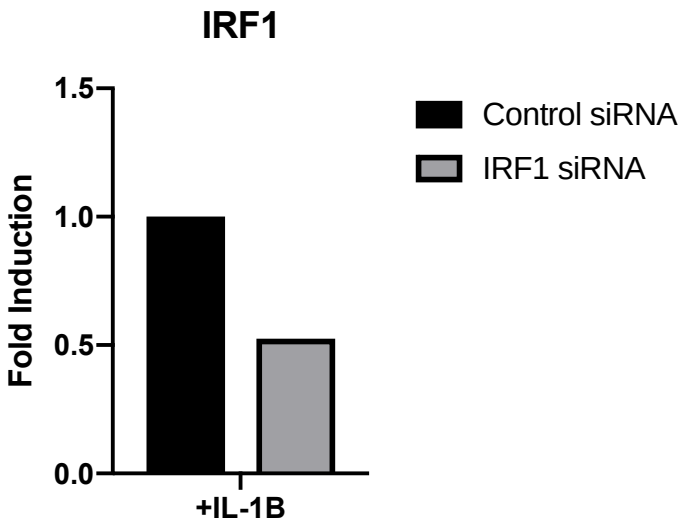

**Figure 5: IRF1 is dispensable for "priming" in astrocytes.** Cells were transfected with either IRF1 siRNA or control siRNA for 2 hours. Cells were stimulated with 20ng/mL IL-1β based on the schedule shown below. Gene expression was analyzed using qPCR. The data shown are normalized to GAPDH expression and all values are compared to IL-1β treated naïve cells, which were set to a value of 100. P values are displayed using two-way ANOVA. LCN2 (n=3), YKL-40 (n=3), and CH25H (n=3)

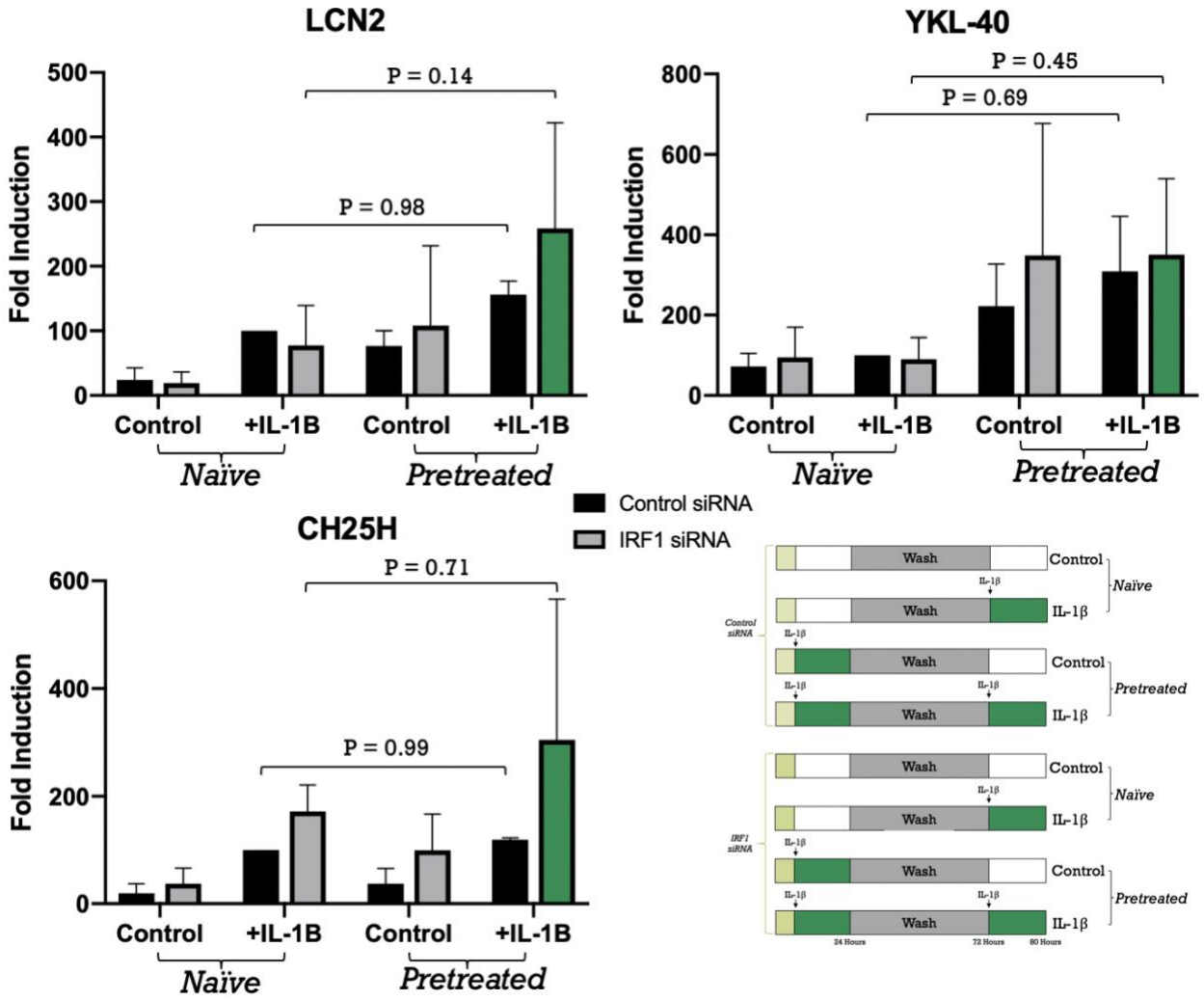

**Type 1 interferon signaling is not responsible for priming.**

Since it was already known that priming was not dependent on IRF1, it was unlikely that it was dependent on type 1 interferon signaling. In order to fully assure that this was the case, AG490, an inhibitor of JAK was used to block this signaling. In these experiments, 50uM AG490 was used to treat cells 30 minutes before IL-1β stimulation. The expression of cells treated with the AG490 was compared to that of the same conditions used in the original priming experiments. Since type 1 interferon signaling is mediated by pSTAT1 and pSTAT2, the first step was to make sure the addition of AG490 was blocking the phosphorylation of these targets. Four groups of astrocytes were used to determine this: control naïve cells, IL-1β stimulated naïve cells, control AG490 treated cells, and IL-1β stimulated AG490 treated cells. Western blot analysis showed that IL-1β induced phosphorylation of STAT1 and STAT2. As expected, the AG490 JAK inhibitor diminished STAT1 phosphorylation and fully blocked STAT2 phosphorylation (Figure 6). The four conditions used in the priming experiments were repeated in the presence or absence of AG490, leading to eight total conditions. If type 1 interferon signaling was responsible for enhancing expression of the primed genes, then the AG490 should abrogate priming. This was not the case, indicating that priming did not rely on type 1 interferon signaling (Figure 7).

**Figure 6: AG490 diminishes STAT1 and STAT2 phosphorylation in astrocytes.** Primary human astrocytes were pretreated with AG490 for 30 minutes and then simulated with 20ng/mL IL-1β for 4 hours, as indicated. The AG490 treatment occurred 30 minutes prior to the IL-1β stimulation that lasted 4 hours. At the end of the experiment, RIPA buffer was placed on the astrocytes and they were scraped off of the plate. The pSTAT1 bands can be found at 91kDa and 84kDa (alpha and beta forms respectively) and the pSTAT2 bands can be found at 113kDa and 97kDa (alpha and beta forms respectively). β-Tubulin is shown as an indicator of equal protein concentration in each lysate and can be found at 50kDa.

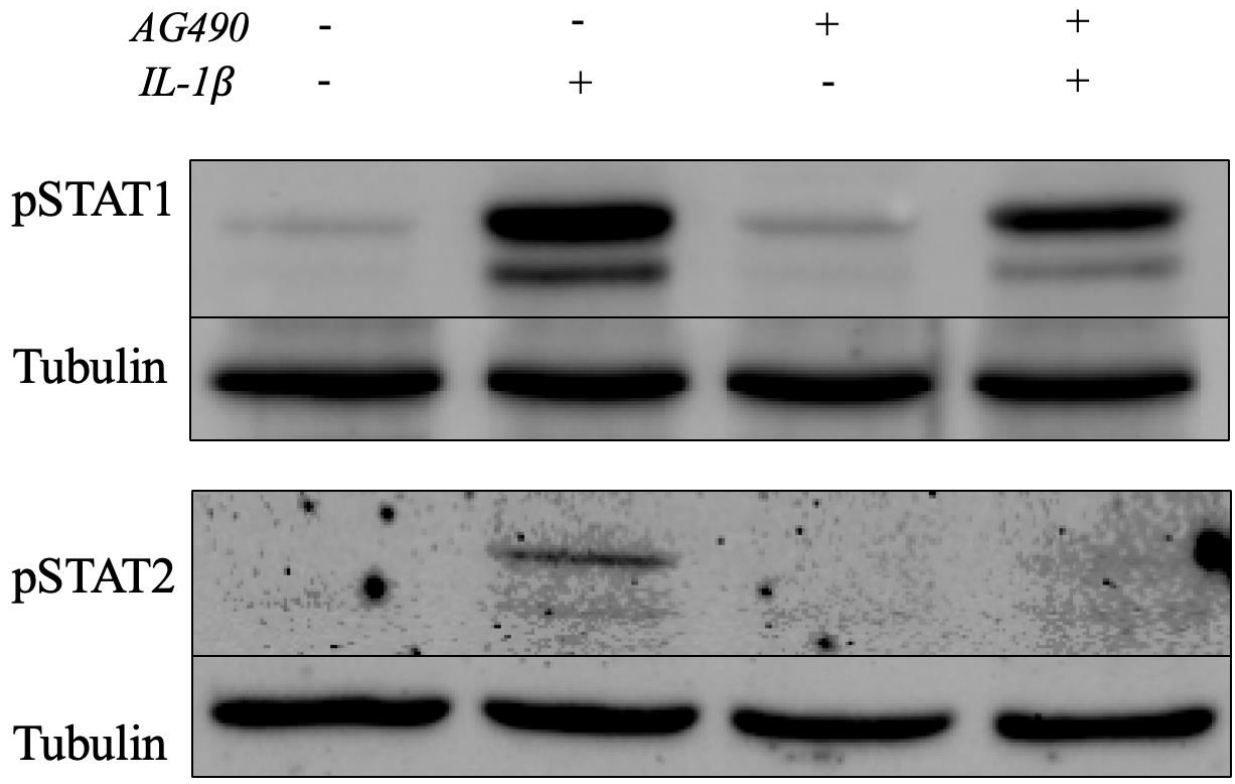

**Figure 7: Blocking JAK-STAT signaling does not abolish "priming".** Bars shown in grey and green represent cells that were treated with AG490 for 30 minutes. IL-1β was given based on the schedule shown below. Gene expression was analyzed using qPCR. The data shown are normalized to GAPDH expression and all values are compared to IL-1β treated naïve cells, which were set to a value of 100. P values are displayed using two-way ANOVA. LCN2 (n=3), YKL-40 (n=3), and CH25H (n=3) showed priming in the presence and absence of AG490.

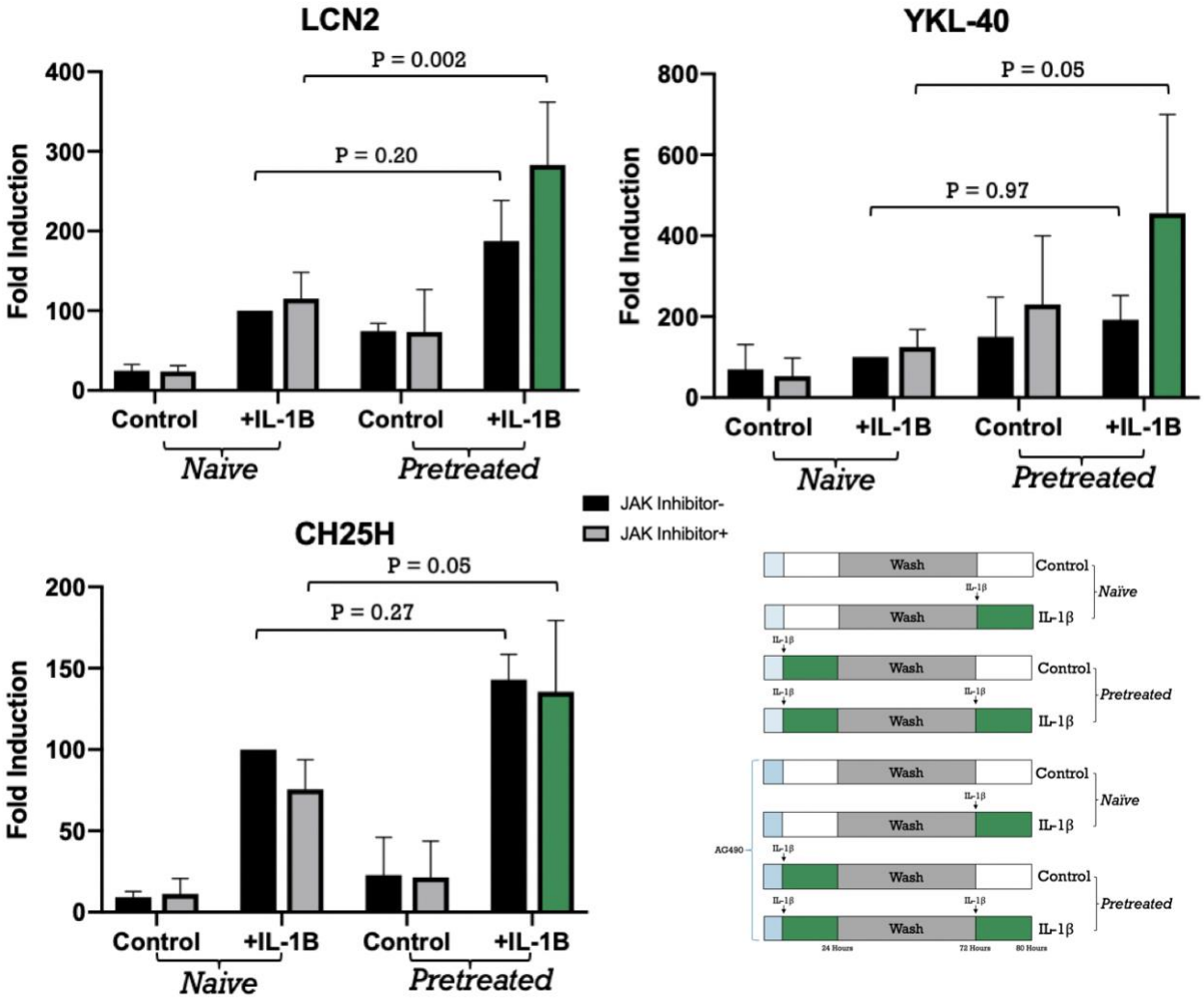

**A secreted factor upregulates both primed and tolerant genes.**

Experiments were performed to evaluate whether priming is mediated by factor(s) secreted by astrocytes. In these experiments, two groups of astrocytes were plated on 6-cm dishes and one was treated with 20 ng/mL IL-1β for an hour while the other was not. The media was then removed and new media was placed to collect secreted factors for 23 hours. The media from the naïve 6-cm dish and the media from the IL-1β treated astrocytes were then placed on new astrocytes. The priming experiment was performed as shown on the schematic (Figure 8). Naïve media and IL-1β -induced media were used instead of the initial IL-1β stimulations. Interestingly, medium collected from IL-1β stimulated cells induced efficient priming of the LCN2, YKL-40, and CH25H genes. In order to prove that this phenomenon was exclusive to the primed genes, the expression of the tolerant genes was examined. Surprisingly, the "tolerant" genes were also "primed" by media from IL-1β stimulated cells. This cannot be explained by the presence of residual IL-1β since these genes undergo tolerance when treated with IL-1β (Figure 9). These experiments suggest that an unknown external factor was causing an increased expression of both the primed and tolerant genes.

**Figure 8: Primed genes are upregulated by a secreted factor.** Cells were treated based on the schedule shown below. Gene expression was analyzed using qPCR. The data shown are normalized to GAPDH expression and all values are compared to IL-1β treated naïve cells, which were set to a value of 100. P values are displayed using 2-way ANOVA. LCN2 (n=2), YKL-40 (n=2), and CH25H (n=2) showed upregulation when given media from cells previously stimulated with IL-1β.

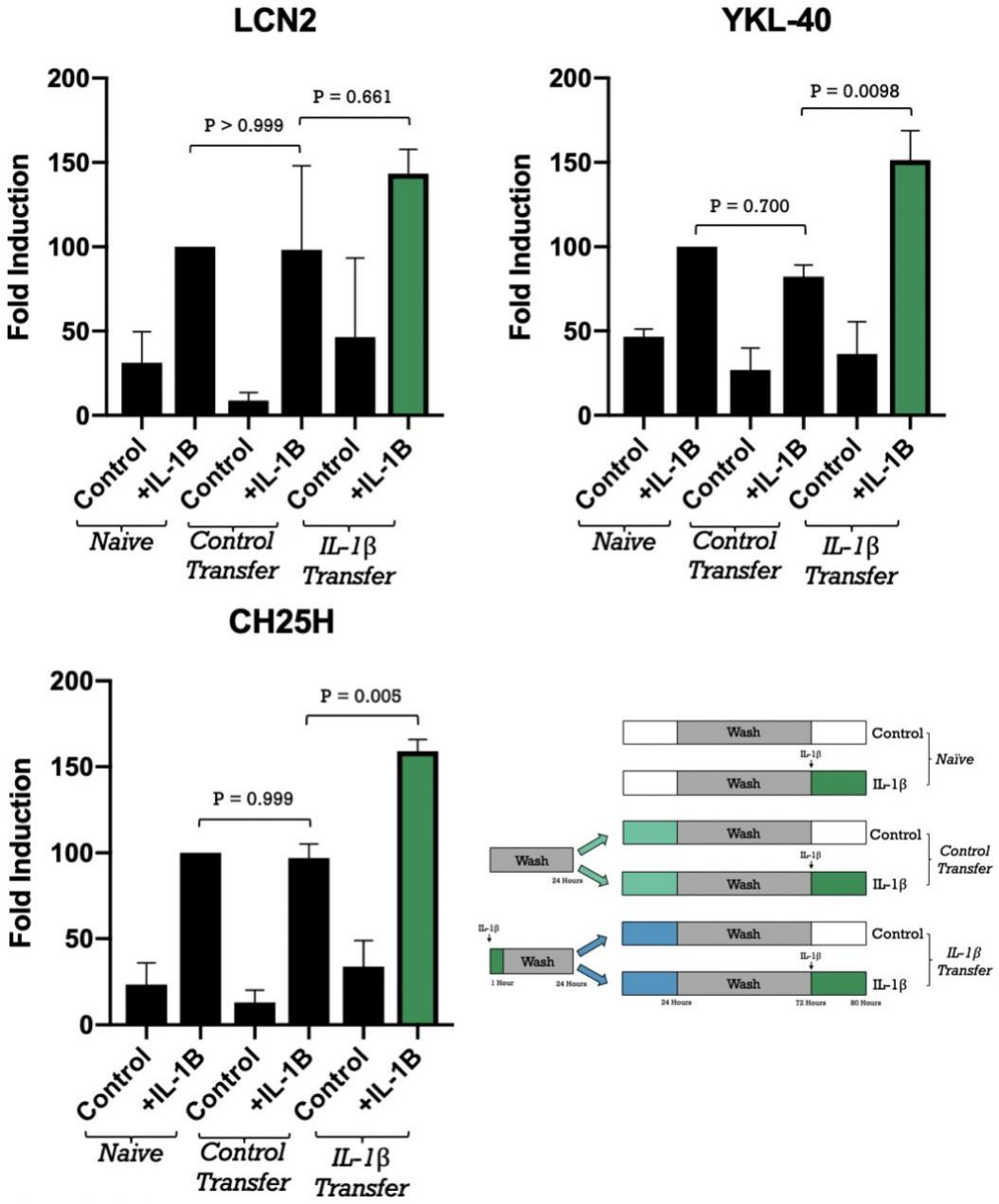

**Figure 9: The secreted factor upregulates "tolerant" genes.** Cells were treated based on the schedule shown below. Gene expression was analyzed using qPCR. The data shown are normalized to GAPDH expression and all values are compared to IL-1β treated naïve cells, which were set to a value of 100. P values are displayed using 2-way ANOVA. LCN2 (n=2), YKL-40 (n=2), and CH25H (n=2) showed upregulation when given media from cells previously stimulated with IL-1β.

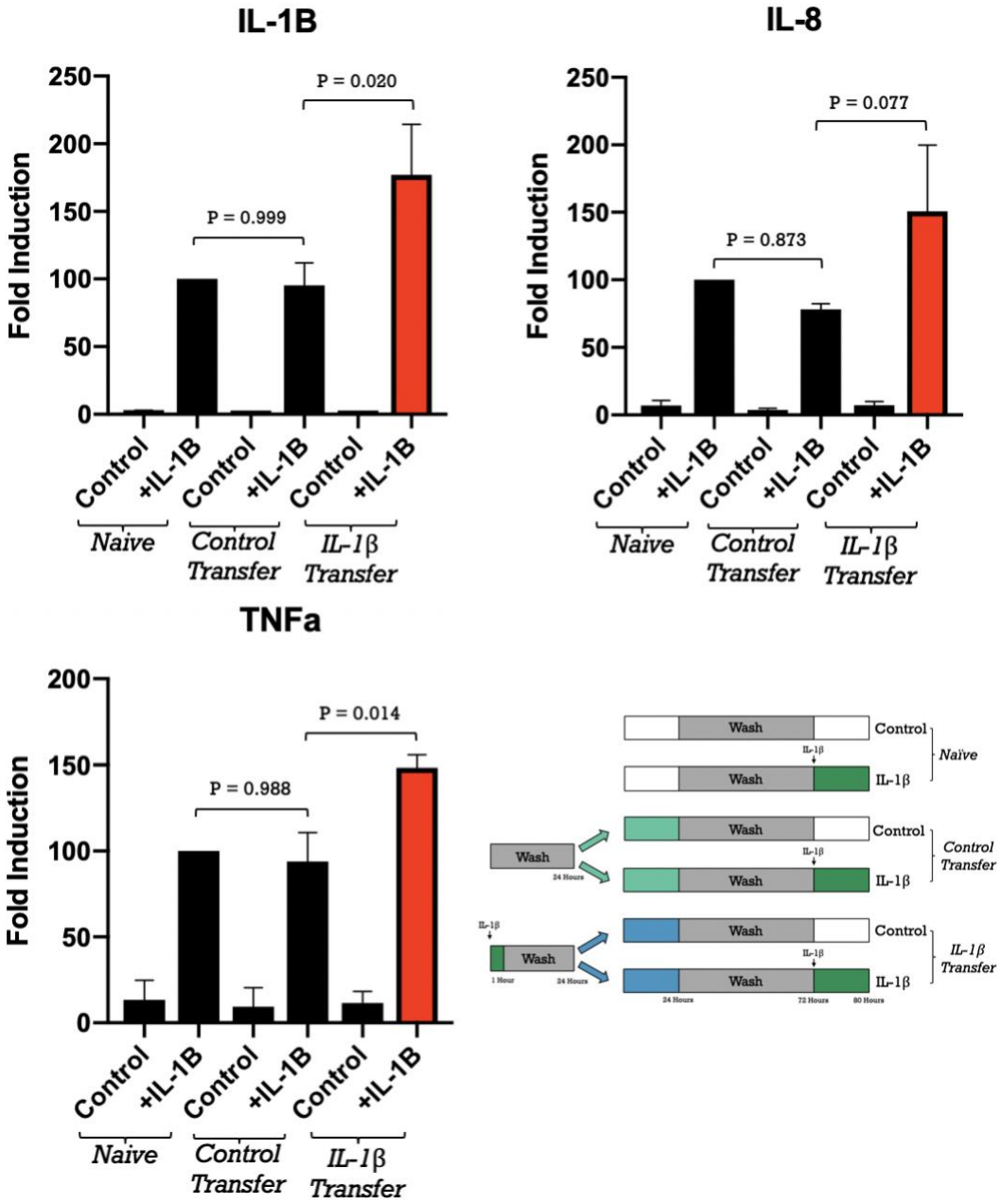

**Deletion of IRF1 from myeloid cells does not protect mice from negative effects of EAE.** Following the experiments involving astrocytes, the role of IRF1 in the brain was explored in vivo. EAE, an experimental method used to model multiple sclerosis, was performed on mice that had cell specific deletions of IRF1. Although the first part of my project was related to astrocytes, GFAP IRF1 Cre mice (astrocyte specific deletion) did not show significant difference in disease severity from the wildtype littermates, so we examined the role of myeloid cells and oligodendrocytes. First, a Cre recombinase system was used to delete IRF1 from myeloid cells in the mice. The notable cells that this affects are the macrophages that infiltrate the CNS during EAE and resident microglia. The graph of EAE scores over time shown below demonstrates that the progression of the disease is not affected by deletion of IRF1 from the myeloid cells of the mice (Figure 10). In order to analyze whether deletion of IRF1 had an effect on gene expression during EAE, gene expression was analyzed using qPCR for 22 genes of interest. Although EAE resulted in a loss of expression of mature oligodendrocyte markers (MBP, PLP1), there was no difference between $I$RF1$^{\Delta Myeloid}$ and WT mice (Figure 11a). EAE attacks the myelin sheath of neurons, formed by the oligodendrocytes, so oligodendrocyte markers can be telling of disease severity. Second, the chemokine and macrophage marker expression was examined (Figure 11b-c). Even though there was lower expression of chemokines in the $I$RF1$^{\Delta Myeloid}$ mice, there were comparable amounts of macrophages being recruited to the area of inflammation in the $I$RF1$^{\Delta Myeloid}$ mice, as shown by their marker expression. The phenotypes of the recruited macrophages were analyzed using M1 and M2 markers (Figure 11d). Out of the M1 markers, iNOS was greatly decrease in the $I$RF1$^{\Delta Myeloid}$ mice, while the CD86 showed little change. This decrease in iNOS suggests that the infiltrating macrophages were less inflammatory in the $I$RF1$^{\Delta Myeloid}$ mice. The M2 markers, IL-10 and Arg1 remained unchanged. Interestingly, there

were lower numbers of pro-inflammatory cytokines present in the $I$RF1$^{\Delta Myeloid}$ mice (Figure 11e). The expression of markers of activated astrocytes and microglia remained unchanged in the $I$RF1$^{\Delta Myeloid}$ mice and their Cre- littermates (Figure 11f-g).

**Figure 10: IRF1$^{\Delta Myeloid}$ mice are not protected from EAE.** Data shown below are averages of the EAE score from Lyz2 Cre- (n = 7) and Lyz2 Cre+ (n = 7) mice. Two-way t-test analysis was used to determine any significant differences between time points for each day following treatment, but no significant values were found. All mice were sacrificed 17 days following treatment.

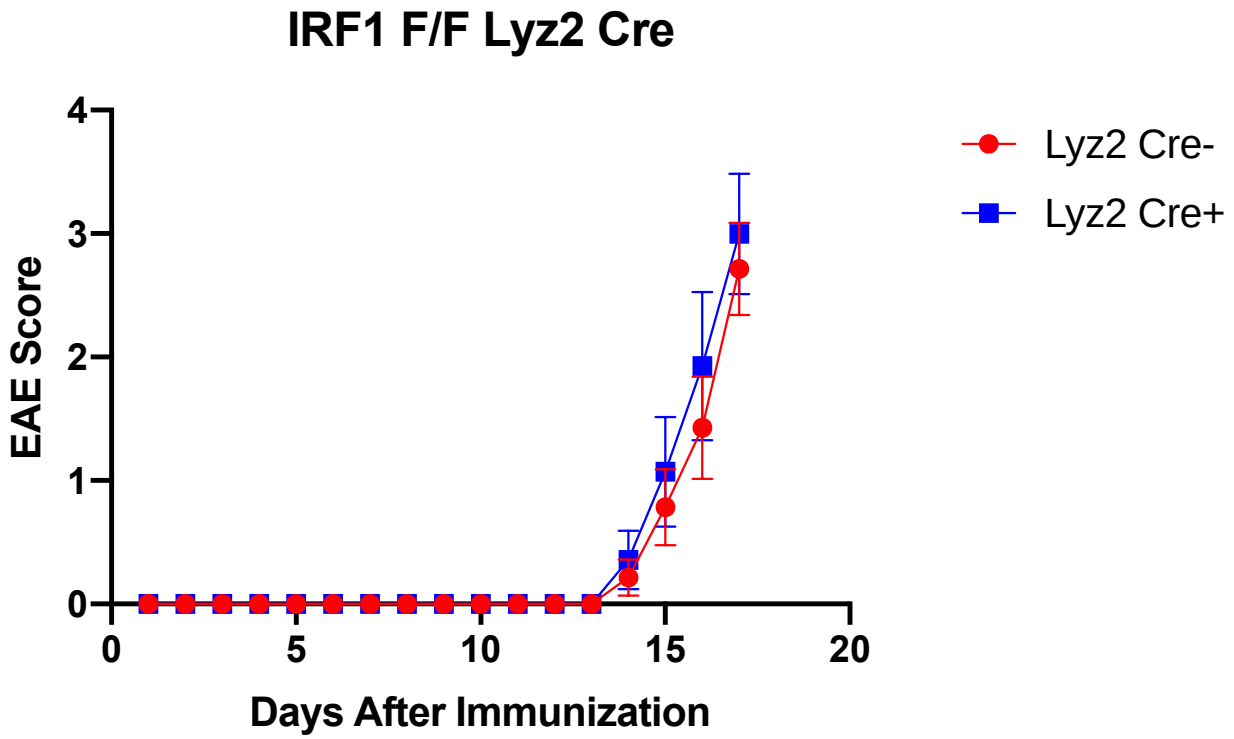

**Figure 11: Deletion of IRF1 from myeloid cells alters gene expression during EAE.** Gene expression in lumbar spinal cords was analyzed using qPCR. All values were normalized using GAPDH expression. The naïve Cre- mice were set to an average of 1 and all other values are set in comparison to those mice. Two-way t-tests between the EAE Cre- and EAE Cre+ mice are shown, except for oligodendrocyte markers, analyzed with one-way ANOVA. Data are organized in the based on their markers: (A) oligodendrocytes, (B) chemokines, (C) infiltrating macrophages, (D) M1 vs M2, (E) cytokines, (F) astrocytes, and (G) microglia. The data are separated by treatment and phenotype: naïve Cre- (n = 4), naïve Cre+ (n = 4), EAE Cre- (n = 5), and EAE Cre+ (n = 4).

A.

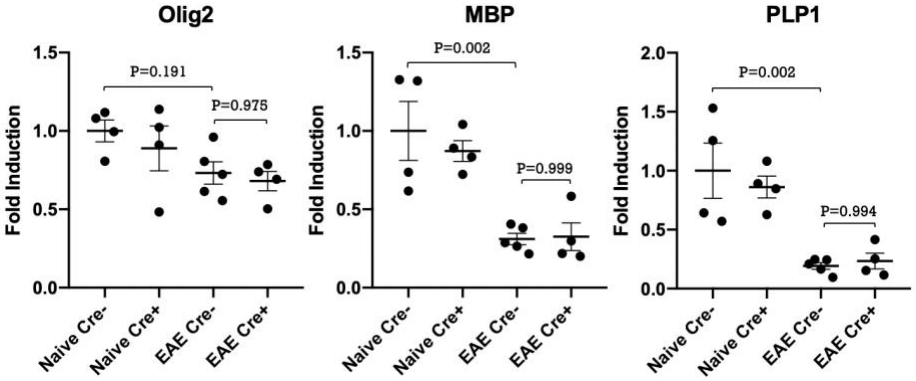


B.

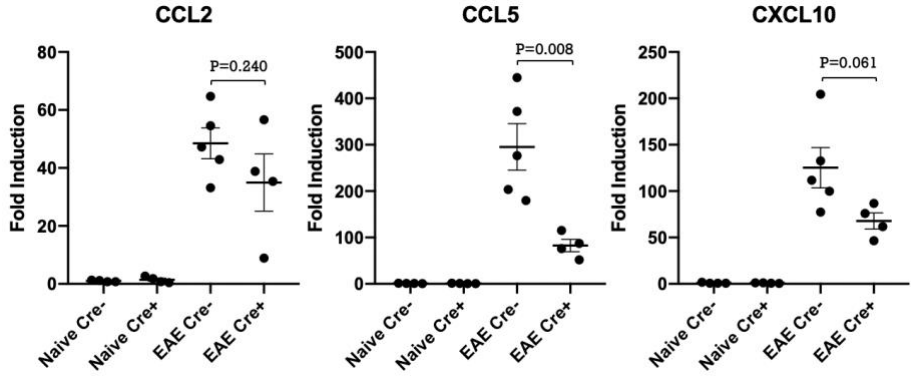

C.

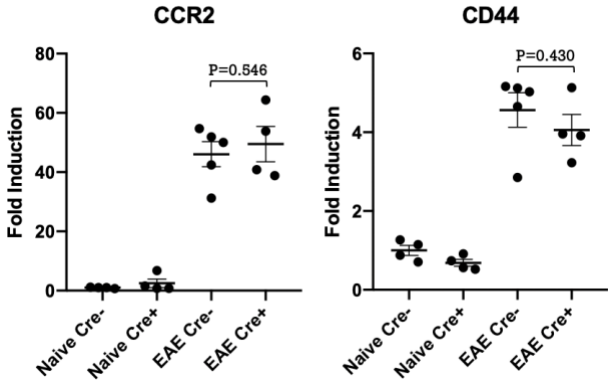
CCR2
CD44
Fold Induction
P=0.546
P=0.430
Naive Cre-
Naive Cre+
EAE Cre-
EAE Cre+

D.

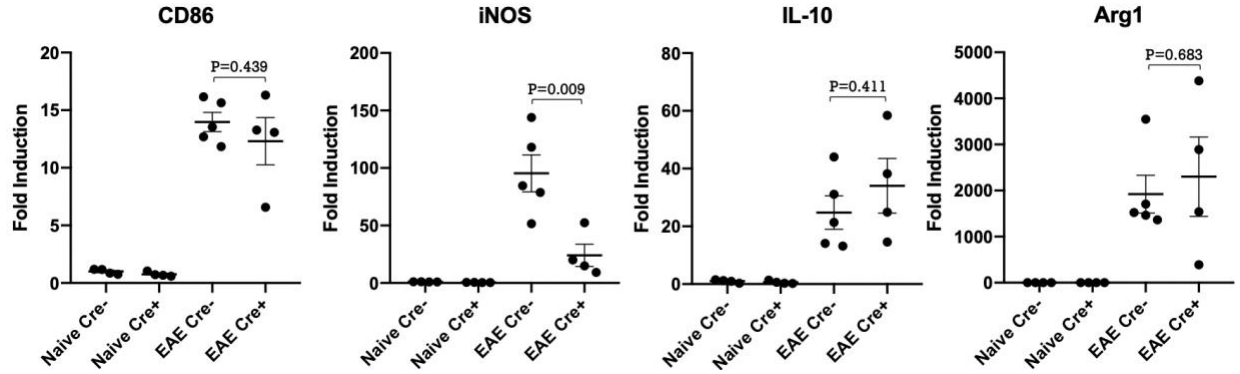
CD86
iNOS
IL-10
Arg1
Fold Induction
P=0.439
P=0.009
P=0.411
P=0.683
Naive Cre-
Naive Cre+
EAE Cre-
EAE Cre+

E.

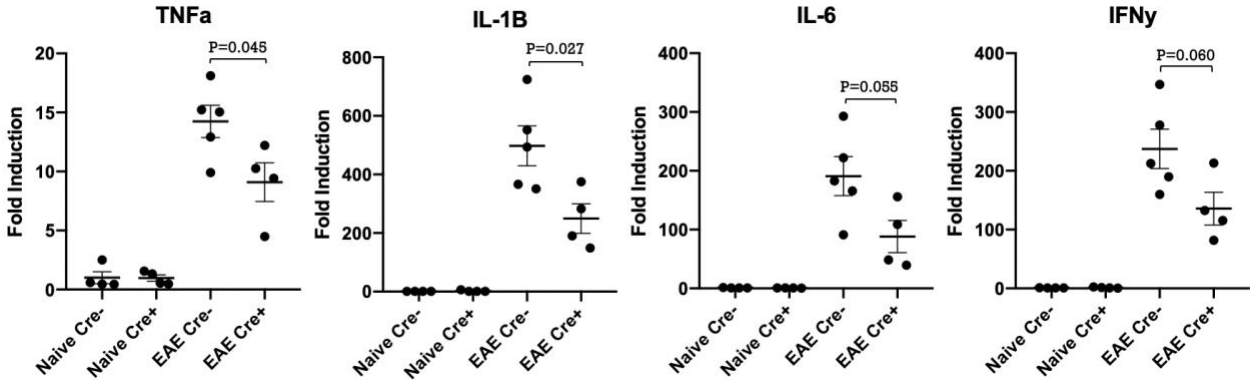
TNFa
IL-1B
IL-6
IFNy
Fold Induction
P=0.045
P=0.027
P=0.055
P=0.060
Naive Cre-
Naive Cre+
EAE Cre-
EAE Cre+

F.

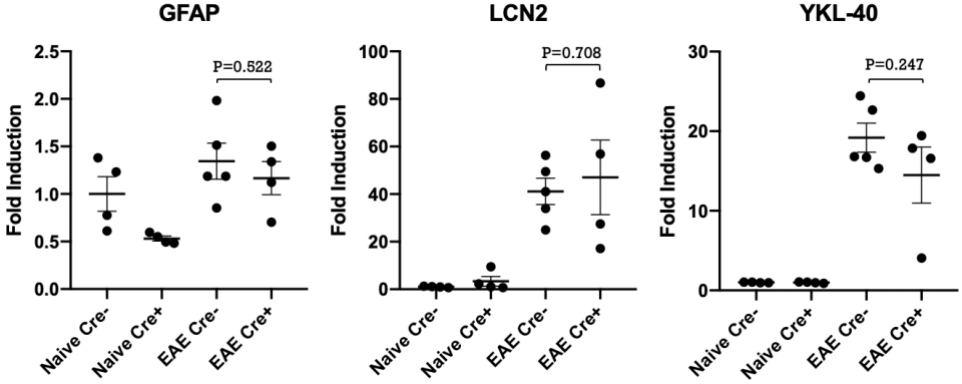
GFAP
LCN2
YKL-40
Fold Induction
P=0.522
P=0.708
P=0.247
Naive Cre-
Naive Cre+
EAE Cre-
EAE Cre+

G.

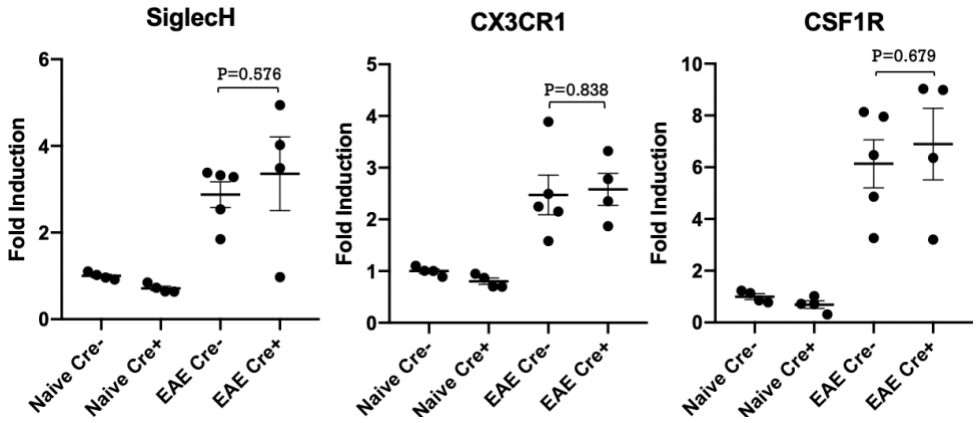
SiglecH
CX3CR1
CSF1R
Fold Induction
P=0.576
P=0.838
P=0.679
Naive Cre-
Naive Cre+
EAE Cre-
EAE Cre+

**Deletion of IRF1 from oligodendrocytes reduces severity of EAE.** The EAE was performed in the same way as for the $I\text{RF1}^{\Delta Oligo}$ mice. A Cre recombinase system, driven by the CNPase promotor, was used to delete IRF1 from oligodendrocytes in the mice. The graph of EAE scores over time shown below demonstrates that the progression of the disease is much less severe for the $I\text{RF1}^{\Delta Oligo}$ mice than their F/F littermates (Figure 12). In order to further analyze this protective feature of IRF1 deletion from oligodendrocytes gene expression was analyzed using qPCR for 22 genes of interest. First, we found that expression of a marker of oligodendrocyte progenitors, Olig2 along with markers of mature oligodendrocytes, MBP and PLP1 was significantly increased in $I\text{RF1}^{\Delta Oligo}$ mice (Figure 13a). These data suggest increased survival of oligodendrocytes during EAE. In the $I\text{RF1}^{\Delta Oligo}$ mice, the chemokine expression was greatly reduced and as a result, it can be seen that less macrophage markers were expressed, indicating decreased recruitment of macrophages (Figure 13b-c). Interestingly, M1 and M2 markers were also much lower in the $I\text{RF1}^{\Delta Oligo}$ mice and this is most likely due to the fact that there are simply less macrophages present at the site of inflammation overall (Figure 13d). These data suggest that the recruited myeloid cells are not polarized and likely represent cells in the "M0" phenotype. The expression of cytokines was also vastly decreased and as you could expect based on this, the astrocytes were far less activated (Figure 13e-f). The expression of microglia markers all stayed the same with the exception of CSF1R (Figure 13g).

**Figure 12: Diminished severity of EAE in IRF1$^{\Delta Oligo}$ mice.** Data shown below are averages of the EAE scores from Lyz2 Cre- (n = 10) and Lyz2 Cre+ (n = 9) mice. Two-way t-test analysis was used to determine any significant differences between time points for each day following treatment, with significant values being found from day 14-16 (* = P <0.05, *** = P < 0.001). All mice were sacrificed 16 days following treatment.

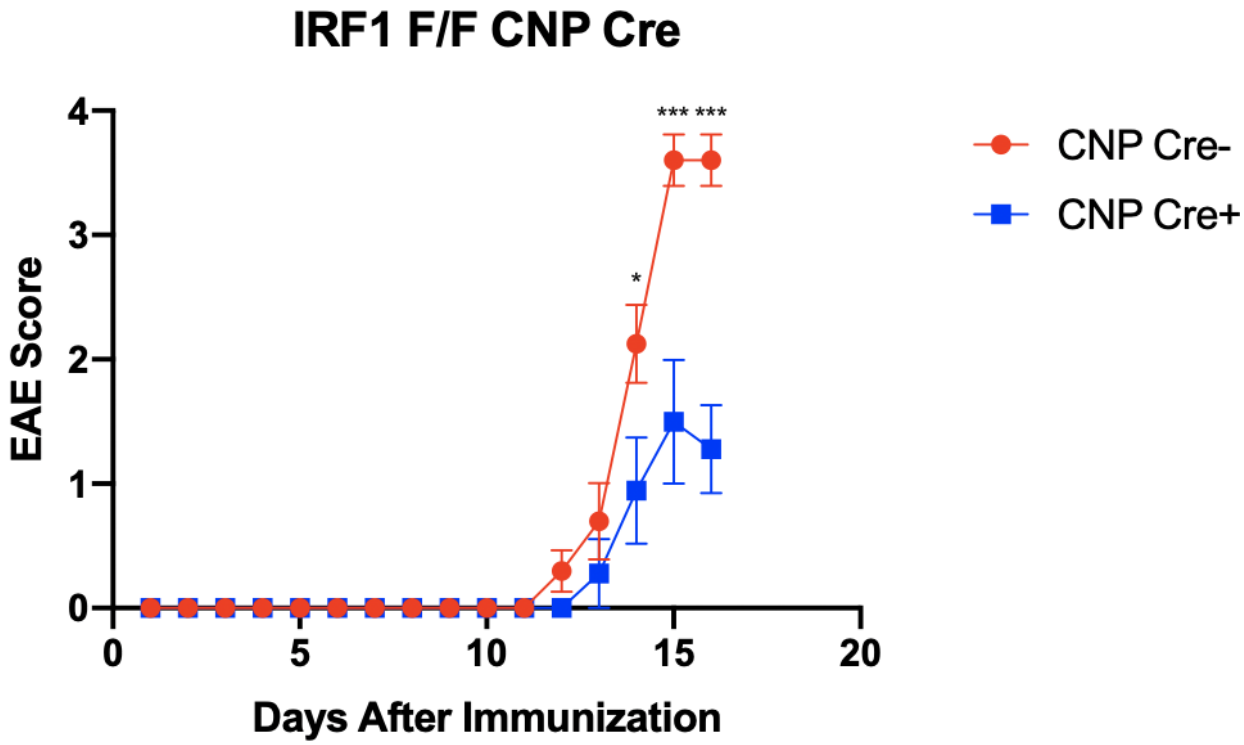

**Figure 13: Deletion of IRF1 from oligodendrocytes greatly alters the gene expression profile.** Gene expression in lumbar spinal cords was analyzed using qPCR. All values were normalized using GAPDH expression. The naïve Cre- mice were set to an average of 1 and all other values are set in comparison to those mice. Two-way t-tests between the EAE Cre- and EAE Cre+ mice are shown. Data are organized in the based on their markers: (A) oligodendrocytes, (B) chemokines, (C) infiltrating macrophages, (D) M1 vs M2, (E) cytokines, (F) astrocytes, and (G) microglia. The data are separated by treatment and phenotype: naïve Cre- (n = 4), naïve Cre+ (n = 4), EAE Cre- (n = 7), and EAE Cre+ (n = 4).

A.

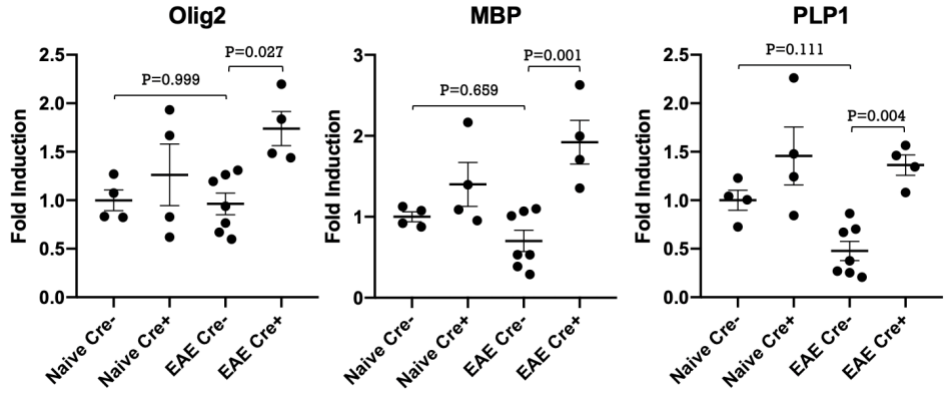


B.

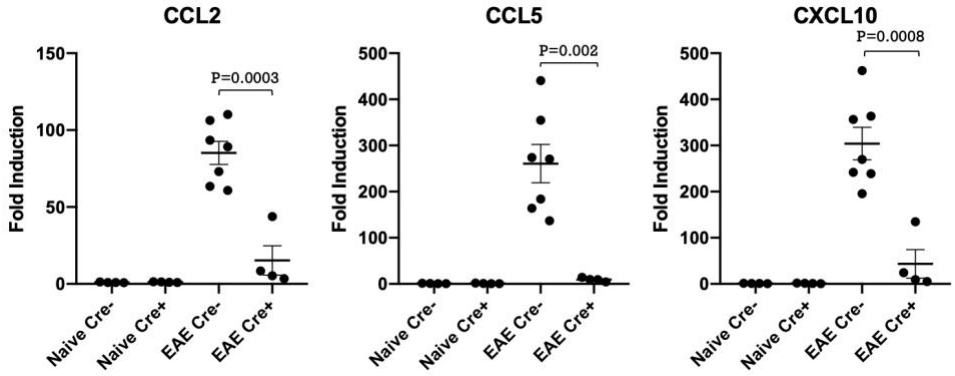

C.

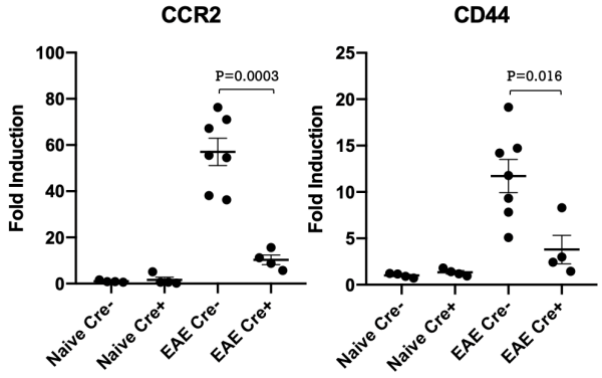
CCR2
P=0.0003
Fold Induction
100
80
60
40
20
0
Naive Cre-
Naive Cre+
EAE Cre-
EAE Cre+
CD44
P=0.016
Fold Induction
25
20
15
10
5
0
Naive Cre-
Naive Cre+
EAE Cre-
EAE Cre+

D.

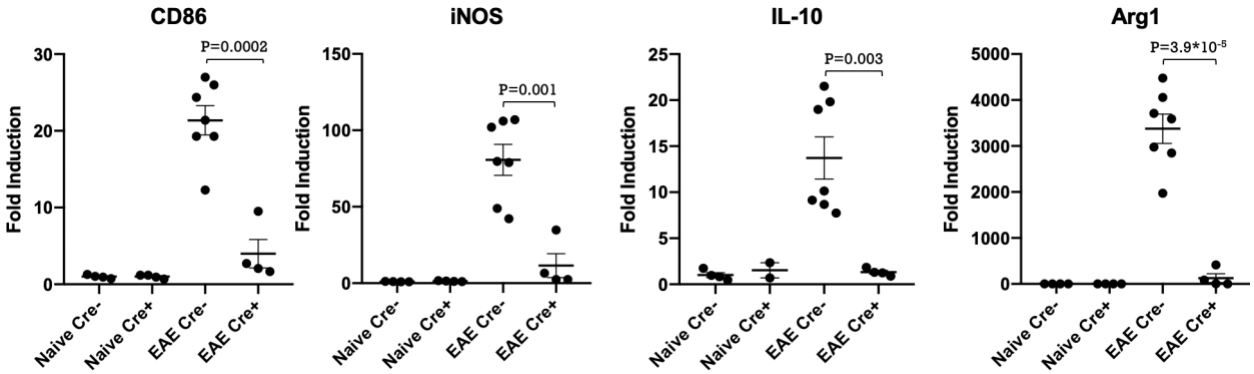
CD86
P=0.0002
Fold Induction
30
20
10
0
Naive Cre-
Naive Cre+
EAE Cre-
EAE Cre+
iNOS
P=0.001
Fold Induction
150
100
50
0
Naive Cre-
Naive Cre+
EAE Cre-
EAE Cre+
IL-10
P=0.003
Fold Induction
25
20
15
10
5
0
Naive Cre-
Naive Cre+
EAE Cre-
EAE Cre+
Arg1
P=3.9*10-5
Fold Induction
5000
4000
3000
2000
1000
0
Naive Cre-
Naive Cre+
EAE Cre-
EAE Cre+

E.

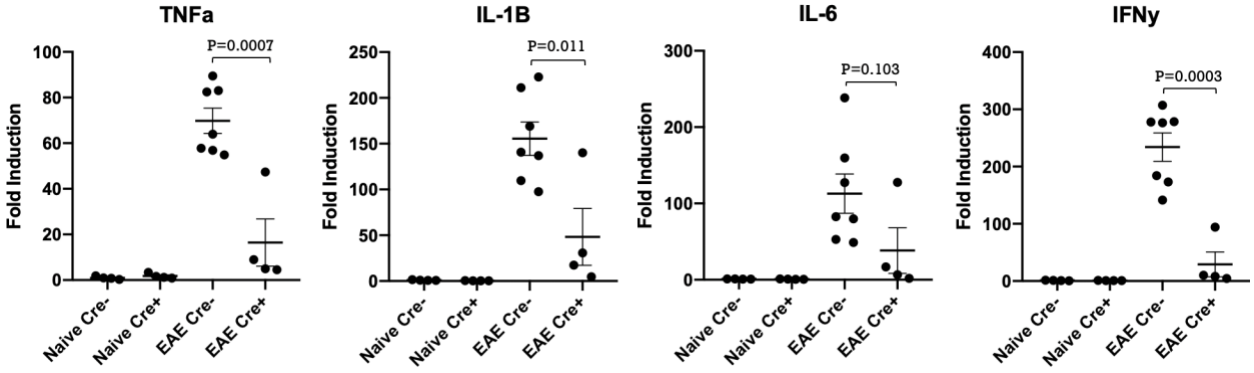
TNFa
P=0.0007
Fold Induction
100
80
60
40
20
0
Naive Cre-
Naive Cre+
EAE Cre-
EAE Cre+
IL-1B
P=0.011
Fold Induction
250
200
150
100
50
0
Naive Cre-
Naive Cre+
EAE Cre-
EAE Cre+
IL-6
P=0.103
Fold Induction
300
200
100
0
Naive Cre-
Naive Cre+
EAE Cre-
EAE Cre+
IFNy
P=0.0003
Fold Induction
400
300
200
100
0
Naive Cre-
Naive Cre+
EAE Cre-
EAE Cre+

F.

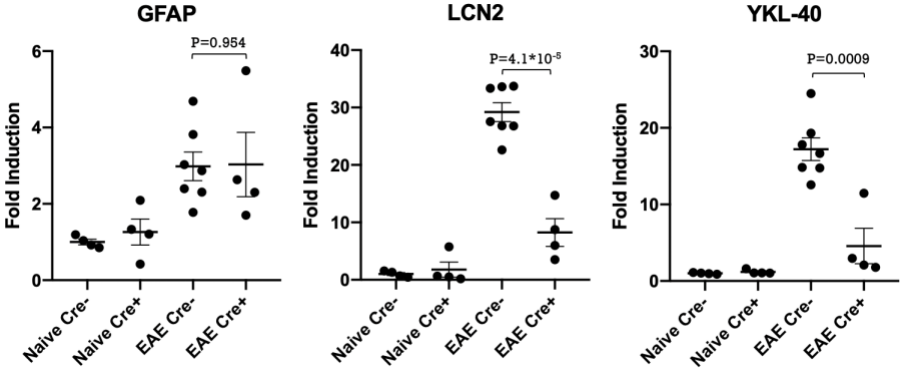
GFAP
P=0.954
Fold Induction
6
4
2
0
Naive Cre-
Naive Cre+
EAE Cre-
EAE Cre+
LCN2
P=4.1*10-5
Fold Induction
40
30
20
10
0
Naive Cre-
Naive Cre+
EAE Cre-
EAE Cre+
YKL-40
P=0.0009
Fold Induction
30
20
10
0
Naive Cre-
Naive Cre+
EAE Cre-
EAE Cre+

G.

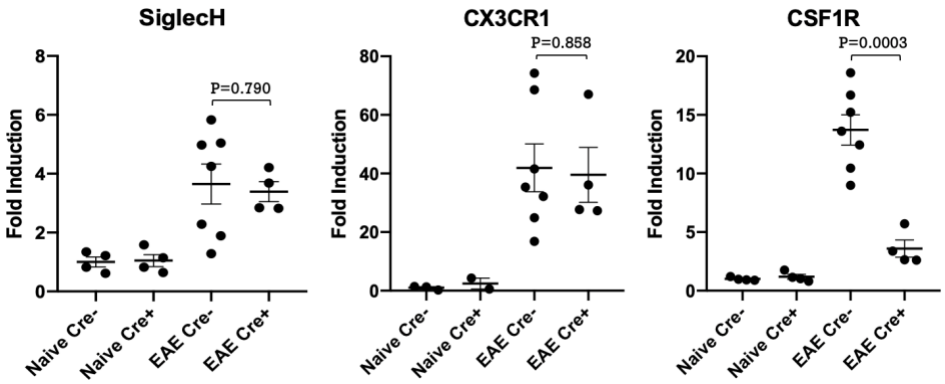
SiglecH
Fold Induction
P=0.790
Naive Cre-
Naive Cre+
EAE Cre-
EAE Cre+
CX3CR1
Fold Induction
P=0.858
Naive Cre-
Naive Cre+
EAE Cre-
EAE Cre+
CSF1R
Fold Induction
P=0.0003
Naive Cre-
Naive Cre+
EAE Cre-
EAE Cre+

## Discussion

Neurodegenerative diseases are a highly prevalent issue in the world, that greatly affect the older population of the world (Johnson, 2015). With an increase of global life expectancy, the amount of people that are in age related risk of developing one of these diseases is rapidly growing. By 2050, the amount of people aged 60 or older is projected to more than double (Wyss-Coray, 2016). With this growing population, the need for better treatment of neurodegenerative diseases is increasing. The neuroinflammation that is associated with these age-related diseases is mediated through the NF-κB pathway, which is not activated at young ages in the brain, but begins to see greater activation in the later ages (Jones et al., 2017). Some of the treatments of neurodegenerative diseases involve the modulation of NF-κB pathway itself and the expression of its targets, so the thorough understanding of the mechanisms that control this pathway are crucial (Khasnavis et al., 2012). Monocytes display adaptive responses in times of multiple activations, where they reduce their inflammatory responses to prevent an over-inflamed state (Nahid et al., 2009). This phenomenon of tolerance can also be found in astrocytes and it plays a very interesting therapeutic target when treatment for neurodegenerative diseases (Beurel, 2011).

In this study, we attempted to determine the mechanism of priming in astrocytes, a feature that results in the upregulation of certain genes following two stimulations with IL-1β within days of each other. Previously, our lab has determined the mechanism for tolerance, a similar phenomenon, that results in the downregulation of pro-inflammatory cytokines following this same back to back IL-1β stimulation. This mechanism, originally proposed to be epigenetic, ended up being regulated through phosphorylation of RelB, which in turn blocks the binding of p65/p50 to the promotors of the cytokine genes (Gupta et al., in press). In our theorized mechanism for priming, we proposed that the upregulation of the genes of interest, many of which were markers of reactive astrocytes,

was mediated by IRF1 and type 1 interferon signaling activating the JAK-STAT pathway. This hypothesis was based on previous findings from our lab that showed induction of IRF1 and activation JAK-STAT signaling in response to IL-1β (Figure 1).

In order to explore the possibilities of mechanisms involved in priming, we first verified it in a set of experiments (Figure 3). This shows that in some manner, the primed genes are becoming more active after initial stimulation. In the experiments following this, we proposed that this activation is mediated by IRF1 and ISGF3, which both translocate to the nucleus. In the experiments exploring involvement of IRF1, we used IRF1 siRNA to knock down the expression of IRF1. We expected to see that this experiment would result in a reduced effect of priming, showing that the mechanism was dependent on IRF1 signaling. The experiments involving IRF1 siRNA showed no reduction in the upregulation of the primed genes, suggesting that IRF1 may not be crucial for priming (Figure 5). Since we knew that IRF1, which induces production of IFN-β, was most likely not involved in priming, type 1 interferon signaling should not be either. In order to confirm this, we explored the involvement of type 1 interferon signaling through the use of a JAK inhibitor, AG490. Indeed, priming was still observed in the presence of AG490 (Figure 7). This suggests that the hypothesis of priming being dependent on IRF1 and type 1 interferon signaling was incorrect.

Since the original hypothesis was proven to not be correct, we decided to look at a broader approach and see if any external factors were responsible for priming. Our data suggests that the primed genes were indeed upregulated by an external factor secreted by astrocytes in response to initial IL-1β stimulation (Figure 8). In order to assure this effect wasn't due to residual IL-1β in the transferred media, expression of the tolerant genes was tested. If residual IL-1β was in the transferred media, we would expect to see a downregulation of the tolerant genes, but this was not

the case. The tolerant genes saw a similar upregulation as was seen in the primed genes (Figure 9). This led us to believe that this external factor was a way of astrocytes to warn surrounding cells that activation is imminent in the near future. Thus, there are two independent mechanisms regulating gene expression in response to subsequent inflammatory signals.

Following the exploration of IRF1's effect on priming of astrocytes in vitro, we analyzed the effect of cell specific IRF1 deletion in a mouse model of multiple sclerosis. The myeloid specific deletion of IRF1 did not serve a protective role, as their disease progressed at a similar rate to their wild-type counterpart (Figure 10). Even though the disease progression was unaffected, their gene expression profiles were altered (Figure 11). The expression of cytokines and chemokines in the $I\text{RF1}^{\Delta Myeloid}$ mice were decreased and the macrophages that were infiltrating the area of inflammation showed a less inflammatory phenotype. Nevertheless, expression of mature oligodendrocyte markers indicated loss of mature oligodendrocytes. The discrepancy between the effects on the molecular and cellular level and the severity of the disease were surprising. However, these discrepancies can be explained by overall high severity in both EAE treatments. The decrease in cytokines and chemokines suggests that IRF1 deletion provides a slight protective effect, so it is possible that a difference in EAE scores may be observed if the EAE treatment was performed at a lower dose. It is known that IRF1 works with the NF-κB pathway to sustain and amplify gene expression in myeloid cells, so it is expected that its deletion would dampen an inflammatory response (Yarilina et al., 2008).

The most exciting data were obtained using $I\text{RF1}^{\Delta Oligo}$ mice, which displayed less severe diseases than their wild-type counterpart (Figure 12). The gene profiles of the $I\text{RF1}^{\Delta Oligo}$ mice were drastically different to the profiles of the wild-type mice (Figure 13). The most important difference was seen in the oligodendrocyte markers, which showed that the oligodendrocytes were

present at much greater numbers. This most likely contributed to the far lower EAE scores seen in the $I$RF1$^{\Delta Oligo}$ mice. Along with the oligodendrocytes being protected, the lumbar spines in these mice seemed to be far less inflamed. The chemokines were secreted at much lower concentrations and as a result, macrophage infiltration was minimal. As would be expected, the cytokines were also secreted at lower levels and as a result, the astrocytes were much less activated. In a study using an overexpression of a dominant negative form of IRF1 in the oligodendrocytes, they observed a similar protective feature during an EAE treatment. This protective feature was attributed to impaired expression of immune and apoptotic genes (Ren et al., 2011). It is likely that in our mouse model, this deletion of IRF1 in oligodendrocytes led to a decrease in apoptotic gene expression during EAE and thus a decrease in oligodendrocyte death.

The deletion of IRF1 from macrophages and oligodendrocytes altered their gene expression, showing just how important IRF1 is to mediate neuroinflammatory effects. IRF1 could be a potential therapeutic target to make decrease the inflammatory effects of neurodegenerative diseases. If IRF1 deletion led to less inflamed environments, inhibition of the NF-κB pathway, leading to decreased IRF1 expression, could slow the progression of these horrible diseases.

Literature Cited


- Alturki, N. A., Shutinoski, B., Gamero, A. M., McComb, S., Joseph, J., Mossman, K. L., Cessford, E. (2014). Type-I interferon signaling through ISGF3 complex is required for sustained Rip3 activation and necroptosis in macrophages. *Proceedings of the National Academy of Sciences*, *111*(31), E3206–E3213.
- Banjara, M., & Ghosh, C. (2017). Sterile Neuroinflammation and Strategies for Therapeutic Intervention. *International Journal of Inflammation*.
- Basu, A., Krady, J. K., & Levison, S. W. (2004). Interleukin-1: A master regulator of neuroinflammation. *Journal of Neuroscience Research*.
- Beurel, E. (2011). HDAC6 regulates LPS-tolerance in astrocytes. *PLoS ONE*, *6*(10).
- Biswas, S. K., & Mantovani, A. (2010). Macrophage plasticity and interaction with lymphocyte subsets: Cancer as a paradigm. *Nature Immunology*.
- Biswas, S. K., & Mantovani, A. (2012). Orchestration of metabolism by macrophages. *Cell Metabolism*.
- Bonneh-Barkay, D., Wang, G., Starkey, A., Hamilton, R. L., & Wiley, C. A. (2010). In vivo CHI3L1 (YKL-40) expression in astrocytes in acute and chronic neurological diseases. *Journal of Neuroinflammation*.
- Chen, G. Y., & Nuñez, G. (2010). Sterile inflammation: Sensing and reacting to damage. *Nature Reviews Immunology*.
- Chen, X., El Gazzar, M., Yoza, B. K., & McCall, C. E. (2009). The NF-κB factor RelB and histone H3 lysine methyltransferase G9a directly interact to generate epigenetic silencing in endotoxin tolerance. *Journal of Biological Chemistry*.
- De Lima, T. M., Sampaio, S. C., Petroni, R., Brigatte, P., Velasco, I. T., & Soriano, F. G. (2014). Phagocytic activity of LPS tolerant macrophages. *Molecular Immunology*.
- De Lima, T. M., Sampaio, S. C., Petroni, R., Brigatte, P., Velasco, I. T., & Soriano, F. G. (2014). Phagocytic activity of LPS tolerant macrophages. *Molecular Immunology*.
- Dobbing, J. (1961). The Blood-Brain Barrier. *Developmental Medicine & Child Neurology*, *3*(6), 610–612.

- Erkkinen, M. G., Kim, M. O., & Geschwind, M. D. (2018). Clinical neurology and epidemiology of the major neurodegenerative diseases. *Cold Spring Harbor Perspectives in Biology*.
- Francescone, R. A., Scully, S., Faibish, M., Taylor, S. L., Oh, D., Moral, L., … Shao, R. (2011). Role of YKL-40 in the Angiogenesis, Radioresistance , and Progression of Glioblastoma. *The Journal of Biological Chemistry*, *286*(17), 15332–15343.
- Gasparini, C., Foxwell, B. M., & Feldmann, M. (2013). RelB/p50 regulates TNF production in LPS-stimulated dendritic cells and macrophages. *Cytokine*, *61*(3), 736–740.
- Griffin, W. S., Stanley, L. C., Ling, C., White, L., MacLeod, V., Perrot, L. J., Araoz, C. (1989). Brain interleukin 1 and S-100 immunoreactivity are elevated in Down syndrome and Alzheimer disease. *Proceedings of the National Academy of Sciences of the United States of America*.
- Gupta, A., Waters, M., Biswas, D., Surace, M., Floros, C., Siebenlist, U., and Kordula, T. (Submitted). Adaptive inflammatory responses of astrocytes are regulated by RelB and its phosphorylation on Serine 472. *Glia*.
- Harikumar, K. B., Yester, J. W., Surace, M. J., Oyeniran, C., Price, M. M., Huang, W. C., Kordula, T. (2014). K63-linked polyubiquitination of transcription factor IRF1 is essential for IL-1-induced production of chemokines CXCL10 and CCL5. *Nature Immunology*.
- Harikumar, K. B., Yester, J. W., Surace, M. J., Oyeniran, C., Price, M. M., Huang, W. C., Kordula, T. (2014). K63-linked polyubiquitination of transcription factor IRF1 is essential for IL-1-induced production of chemokines CXCL10 and CCL5. *Nature Immunology*.
- Hayden, M. S. (2012). A less-canonical, canonical NF-κB pathway in DCs. *Nature Immunology*.
- Hoeksema, M. A., & de Winther, M. P. J. (2016). Epigenetic Regulation of Monocyte and Macrophage Function. *Antioxidants & Redox Signaling*.
- Hoesel, B., & Schmid, J. A. (2013). The complexity of NF-κB signaling in inflammation and cancer. *Molecular Cancer*.
- Johnson, D. E., O'Keefe, R. A., & Grandis, J. R. (2018). Targeting the IL-6/JAK/STAT3 signalling axis in cancer. *Nature Reviews Clinical Oncology*, *15*(4), 234–248.

- Johnson, I. P. (2015). Age-related neurodegenerative disease research needs aging models. *Frontiers in Aging Neuroscience*. https://doi.org/10.3389/fnagi.2015.00168
- Jones, S. V., & Kounatidis, I. (2017). Nuclear factor-kappa B and Alzheimer disease, unifying genetic and environmental risk factors from cell to humans. *Frontiers in Immunology*, *8*(DEC).
- Khasnavis, S., Jana, A., Roy, A., Mazumder, M., Bhushan, B., Wood, T., Pahan, K. (2012). Suppression of nuclear factor-κB activation and inflammation in microglia by physically modified saline. *Journal of Biological Chemistry*, *287*(35), 29529–29542.
- Kjaergaard, A. D., Johansen, J. S., Bojesen, S. E., & Nordestgaard, B. G. (2016). Role of inflammatory marker YKL-40 in the diagnosis, prognosis and cause of cardiovascular and liver diseases. *Critical Reviews in Clinical Laboratory Sciences*.
- Kordula, T., Rydel, R. E., Brigham, E. F., Horn, F., Heinrich, P. C., & Travis, J. (1998). Oncostatin M and the interleukin-6 and soluble interleukin-6 receptor complex regulate α1-antichymotrypsin expression in human cortical astrocytes. *Journal of Biological Chemistry*.
- Lee, S., Jha, M. K., & Suk, K. (2015). Lipocalin-2 in the Inflammatory Activation of Brain Astrocytes. *Critical Reviews in Immunology*, *35*(1), 77–84.
- Lim, C. P., & Cao, X. (2006). Structure, function, and regulation of STAT proteins. *Molecular BioSystems*.
- Liu, T., Zhang, L., Joo, D., & Sun, S.-C. (2017). NF-κB signaling in inflammation. *Signal Transduction and Targeted Therapy*.
- Liu, T., Zhang, L., Joo, D., & Sun, S.-C. (2017). NF-κB signaling in inflammation. *Signal Transduction and Targeted Therapy*.
- Llorens, F., Thüne, K., Tahir, W., Kanata, E., Diaz-Lucena, D., Xanthopoulos, K., … Zerr, I. (2017). YKL-40 in the brain and cerebrospinal fluid of neurodegenerative dementias. *Molecular Neurodegeneration*.
- Locati, M., Mantovani, A., & Sica, A. (2013). Macrophage Activation and Polarization as an Adaptive Component of Innate Immunity. In *Advances in Immunology*.
- Mages, J., Dietrich, H., & Lang, R. (2008). A genome-wide analysis of LPS tolerance in macrophages. *Immunobiology*.

- March, C. J., Mosley, B., Larsen, A., Cerretti, D. P., Braedt, G., Price, V., … Kronheim, S. R. (1985). Cloning, sequence and expression of two distinct human interleukin-1 complementary DNAs. *Nature*.
- Millet, P., McCall, C., & Yoza, B. (2013). RelB: an outlier in leukocyte biology. *Journal of Leukocyte Biology*.
- Moynagh, P. N. (2005). The interleukin-1 signalling pathway in astrocytes: A key contributor to inflammation in the brain. *Journal of Anatomy*.
- Nahid, M. A., Pauley, K. M., Satoh, M., & Chan, E. K. L. (2009). miR-146a is critical for endotoxin-induced tolerance: Implication in innate immunity. *Journal of Biological*
- Ransohoff, R. M. (2002). The Chemokine System in Neuroinflammation: An Update. *The Journal of Infectious Diseases*.
- Rawlings, J. S. (2004). The JAK/STAT signaling pathway. *Journal of Cell Science*, *117*(8), 1281–1283.
- Reboldi, A., Dang, E. V., McDonald, J. G., Liang, G., Russell, D. W., & Cyster, J. G. (2014). 25-hydroxycholesterol suppresses interleukin-1-driven inflammation downstream of type I interferon. *Science*.
- Reitz, C., Brayne, C., & Mayeux, R. (2011). Epidemiology of Alzheimer disease. *Nature Reviews Neurology*.
- Ren, Z., Wang, Y., Tao, D., Goswami, R., Balabanov, R., Liggett, T., … Stefoski, D. (2011). Overexpression of the Dominant-Negative Form of Interferon Regulatory Factor 1 in Oligodendrocytes Protects against Experimental Autoimmune Encephalomyelitis.
- Schmitz, F., Heit, A., Guggemoos, S., Krug, A., Mages, J., Schiemann, M., … Wagner, H. (2007). Interferon-regulatory-factor 1 controls Toll-like receptor 9-mediated IFN-β production in myeloid dendritic cells. *European Journal of Immunology*.
- Shih, V. F. S., Davis-Turak, J., MacAl, M., Huang, J. Q., Ponomarenko, J., Kearns, J. D., Hoffmann, A. (2012). Control of RelB during dendritic cell activation integrates canonical and noncanonical NF-κB pathways. *Nature Immunology*.
- Sofroniew, M. V. (2015). Astrogliosis. *Cold Spring Harbor Perspectives in Biology*.
- Sofroniew, M. V., & Vinters, H. V. (2010). Astrocytes: Biology and pathology. *Acta Neuropathologica*, *119*(1), 7–35.

- Song, J., & Kim, O. Y. (2018). Perspectives in Lipocalin-2 : Emerging Biomarker for Medical Diagnosis and Prognosis for Alzheimer's Disease, *7*(1), 1–10.
- Steinman, L. (2008). Nuanced roles of cytokines in three major human brain disorders. *Journal of Clinical Investigation*.
- Sun, S. C., Chang, J. H., & Jin, J. (2013). Regulation of nuclear factor-κB in autoimmunity. *Trends in Immunology*.
- Wyss-Coray, T. (2016). Ageing, neurodegeneration and brain rejuvenation. *Nature*.
- Yamaoka, K., Saharinen, P., Pesu, M., Holt III, V., Silvennoinen, O., J. J. O. (1977). The Janus Kinases. *ISA Trans.*, *16*, 53–57. https://doi.org/10.1186/gb-2004-5-12-253
- Yanai, H., Negishi, H., & Taniguchi, T. (2012). The IRF family of transcription factors. *OncoImmunology*, *1*(8), 1376–1386.
- Yarilina, A., Park-Min, K. H., Antoniv, T., Hu, X., & Ivashkiv, L. B. (2008). TNF activates an IRF1-dependent autocrine loop leading to sustained expression of chemokines and STAT1-dependent type I interferon-response genes. *Nature Immunology*.
- Yarilina, A., Park-Min, K. H., Antoniv, T., Hu, X., & Ivashkiv, L. B. (2008). TNF activates an IRF1-dependent autocrine loop leading to sustained expression of chemokines and STAT1-dependent type I interferon-response genes. *Nature Immunology*.
- Zhou, H., Xie, S.-J., Xu, H., Zhang, Y., Zheng, M.-N., Yang, J.-H., Qu, L.-H. (2019). MicroRNA-122 supports robust innate immunity in hepatocytes by targeting the RTKs/STAT3 signaling pathway. *ELife*, *8*, 1–26.
- Zlokovic, B. V. (2008). The Blood-Brain Barrier in Health and Chronic Neurodegenerative Disorders. *Neuron*.

## Vita

Andrew Hoskins was born in Fairfax, Virginia on April 19th, 1995. He lived in Virginia for his whole life, where he stayed for his undergraduate degree in Chemistry with Specialization in Biochemistry from the University of Virginia. Following graduation, he began the Graduate Certificate Program at Virginia Commonwealth University to strengthen his application for medical school, however began to realize a growing interest for chemistry and a decreasing interest for medicine. Following completion of the Graduate Certificate program, he transferred into the Biochemistry Master's program at Virginia Commonwealth University. Upon graduation, he will move back to Northern Virginia to seek out work in the chemistry industry. He hopes that he can help discover ways of treating both neurodegenerative diseases and various types of cancer while in industry.